SUPPORTING INFORMATION

Nanocrystal-ligands interaction deciphered: the influence of HSAB and pKa in the case of luminescent ZnO

Yohan Champouret,[+] Grégory Spataro,[+] Yannik Coppel, Fabienne Gauffre*, and Myrtil L. Kahn*

1. 2D plot analysis

We recently propose the analysis of nanoparticle size through a simple 2D plot in order to extract the correlation between length and width in a collection or a mixture of anisotropic particles.[1] Compared to the usual statistics on the length associated with a second and independent statistical analysis of the width, this simple plot easily points out the various types of nanoparticles and their (an)isotropy. For each class of nano-objects, the relationship between width and length (*i.e.*, the strong or weak correlations between these two parameters) suggests information concerning the nucleation/growth processes. It allows one to follow the effect on the shape and size distribution of physical or chemical processes such as simple ripening. Figure SI 1a corresponds to small nanoparticles of 6.8 (0.7) nm which could be considered as isotropic (aspect ratio close to 1); the point cloud is located in the median curve, and Figure SI 1b corresponds to a size distribution of ZnO NPs where the width is more or less constant (4.5 (0.5) nm) and the length of the nanorods is totally independent on the width and is spread over the 10 – 130 nm range (aspect ratio >> 1), mean diameter is equal to 44 (23). Note that all the mean size values of the nanoparticles are given including the standard deviation values in brackets.

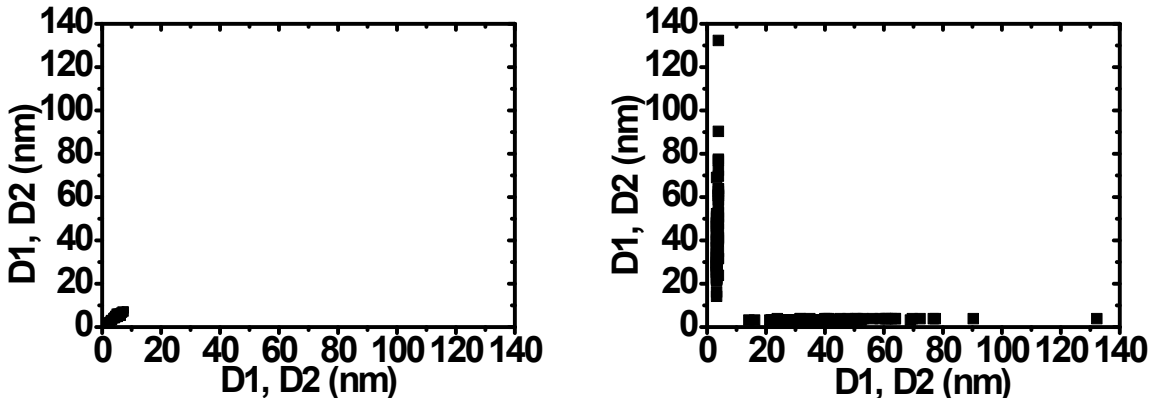

Figure SI1: 2D plots extract from the TEM pictures of isotropic (left) and anisotropic (right) ZnO Ncs.

From the TEM measurements, we calculated the basal, lateral, and total surface per unit of volume, for isotropic Ncs and rods, assuming that Ncs have a cylindrical shape (Table SI1):

	Basal surface (nm^2/nm^3)	Lateral surface (nm^2/nm^3)	Total surface (nm^2/nm^3)
Isotropic	0.31	0.84	1.15
Rods	0.05	0.87	0.92

Table SI1: Basal, lateral, and total surface per unit of volume, for isotropic Ncs and rods calculated from TEM images assuming a cylindrical shape.

2. Optical characterization

Isotropic and anisotropic ZnO NPs display typical UV-visible absorption spectra with a strong absorption between 300 - 375 nm (≈ 3.31 eV - 4.14 eV) with $\lambda_{1/2}$ = 363 nm for both samples (where $\lambda_{1/2}$ is the inflection point calculated by differentiation of the absorption spectrum or the wavelength at which the absorption is half of that at the excitonic peak or shoulder) (Figure SI 2).[2] This absorption is in agreement with that of nano-sized particles of ZnO displaying a band gap of ≈ 3.40 eV (365 nm).

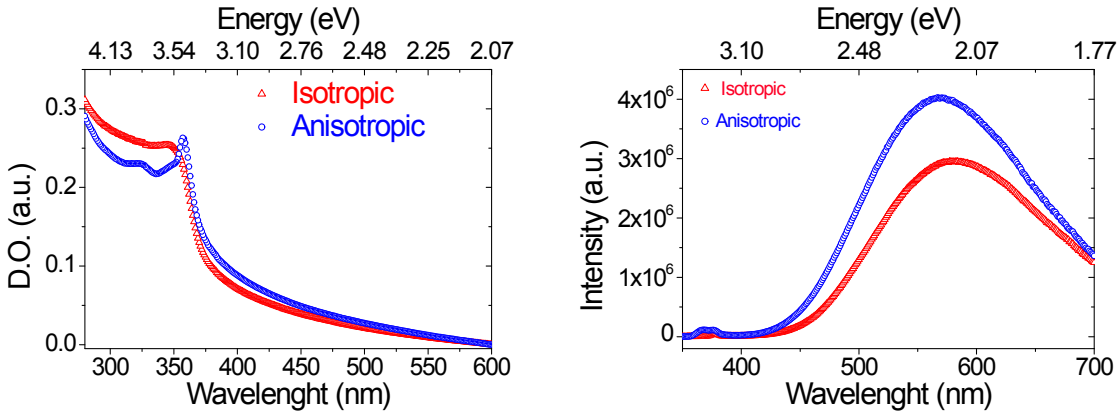

Figure SI2: Absorbance (left) and photoluminescence emission (right) spectra of isotropic and anisotropic ZnO NPs dispersed in THF with $[C]_{S1} = [C]_{S2} = 4 \times 10^{-4}$ mol.L^{-1}.

Table SI2 Summary of size, absorbance and emission properties of isotropic and anisotropic ZnO NPs

Shape of NPs	Diameter size (nm)	$\lambda_{1/2}$	Emission maximum
Isotropic	6.8 (0.7)	363 nm (≈ 3.42 eV)	580 nm (≈ 2.14 eV)
Anisotropic	33 (8) × 4.5 (0.5)	363 nm (≈ 3.42 eV)	570 nm (≈ 2.18 eV)

3. Luminescence properties in the presence of organic substrates

Alkyl-thiol: Figure SI 3 illustrates the decrease of the emission intensity of the ZnO Ncs with increasing concentration of DDT from 4 to 160 µmol.L^{-1}. No wavelength shifts were observed for both UV-Vis and emission spectra during the time of the experiment. For the isotropic ZnO Ncs, the decrease of the emission intensity reached a plateau when ≈ 70 µmol.L^{-1} of DDT was added (0.175 – 0.2 equiv. of DDT), but more importantly, the emission intensity

was not completely quenched and 30% of the emission remained ($I/I_0 \approx 30\%$, I_0 and I represent the intensity before and after addition of DDT). Regarding the anisotropic ZnO NPs, the decrease of the emission intensity followed the one observed for isotropic NPs with $I/I_0 \approx 30\%$, however the plateau occurs more quickly after the introduction of 50 $\mu mol.L^{-1}$ of DDT (0.125 – 0.15 equiv. of DDT).

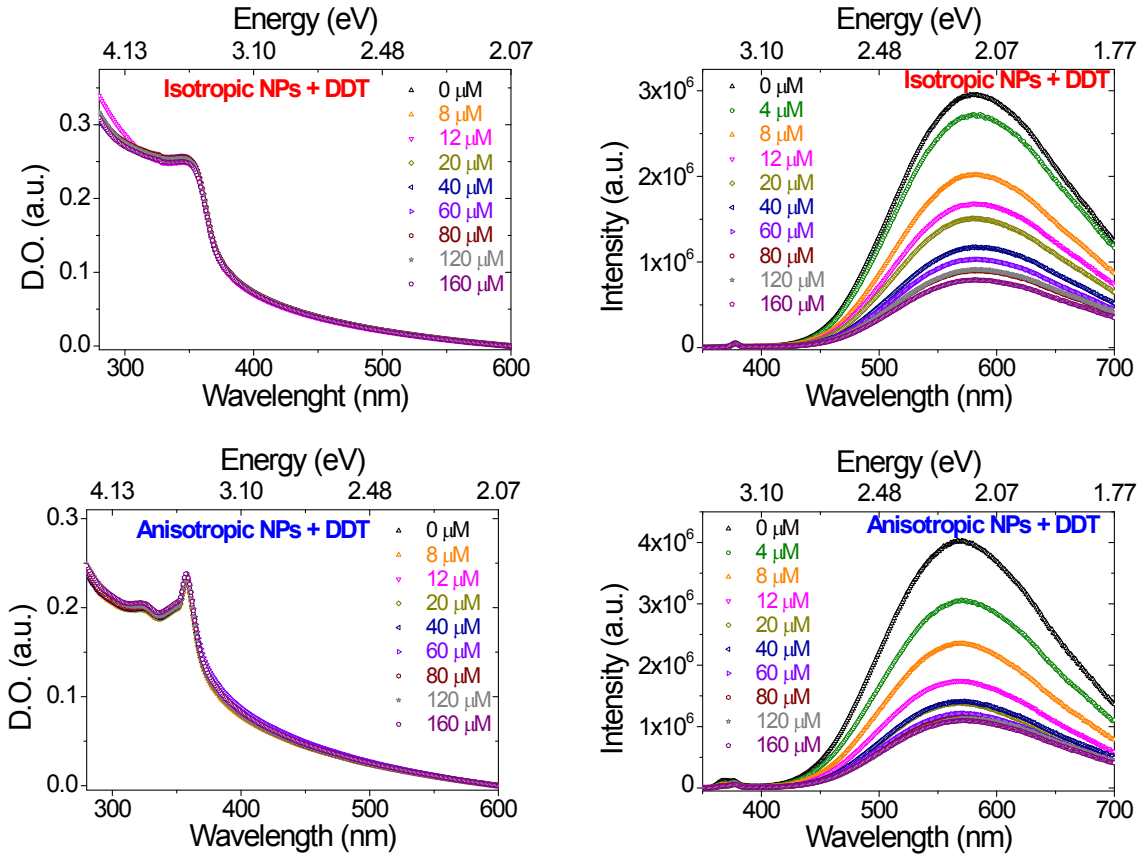

Figure SI3: Absorption and emission spectra of isotropic and anisotropic ZnO NPs in the presence of an increasing amount of dodecanethiol (DDT).

When a shorter alkyl chain bearing a thiol group was used (octanethiol, OT), we observed for both isotropic and anisotropic NPs a similar decreases of the emission intensity upon addition of OT than the one obtained with DDT (Figure SI4). These results showed that the length of the organic molecule does not affect the surface passivation of ZnO Ncs with plateau observed around 70 $\mu mol.L^{-1}$ of OT added for isotropic NPs (plateau with $I/I_0 \approx 30\%$) and 50 $\mu mol.L^{-1}$ for anisotropic NPs (plateau with $I/I_0 \approx 30\%$). It is important to note that the reproducibility of the decrease of the intensity of ZnO Ncs upon addition of alkyl-thiol was not consistent when the stock solutions of ZnO Ncs were used after one week. Indeed, we observed through NMR experiments the formation of carbamate at the surface of the NPs when the solution was kept in air. This observation has been already reported in the literature

and it was suggested that the amine reacts with carbon dioxide following the reaction $2RNH_2 + CO_2 \rightarrow RNHCO_2^- + RNH_3^+$.[3] We believe that the passivation of the surface of ZnO Ncs by addition of alkyl-thiol molecules was highly influenced by the presence of carbamate ligand and could explain the difficulty to reproduce these experiments after one week.

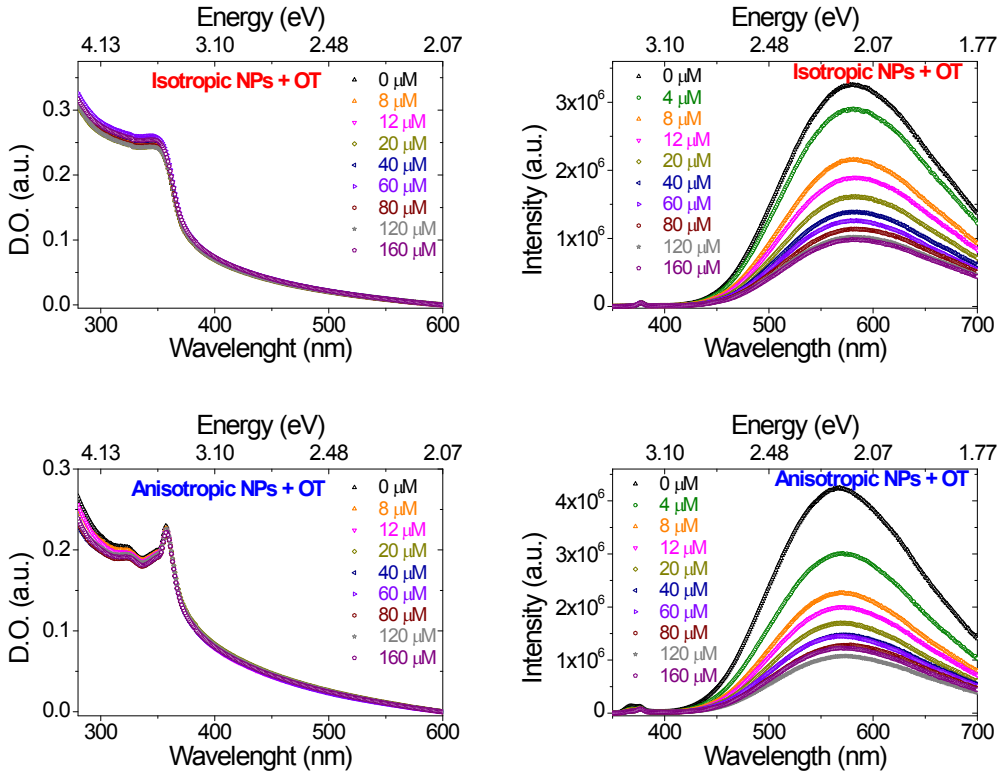

Figure SI 4: Absorption and emission spectra of isotropic and anisotropic ZnO NPs in the presence of an increasing amount of octanethiol (OT)

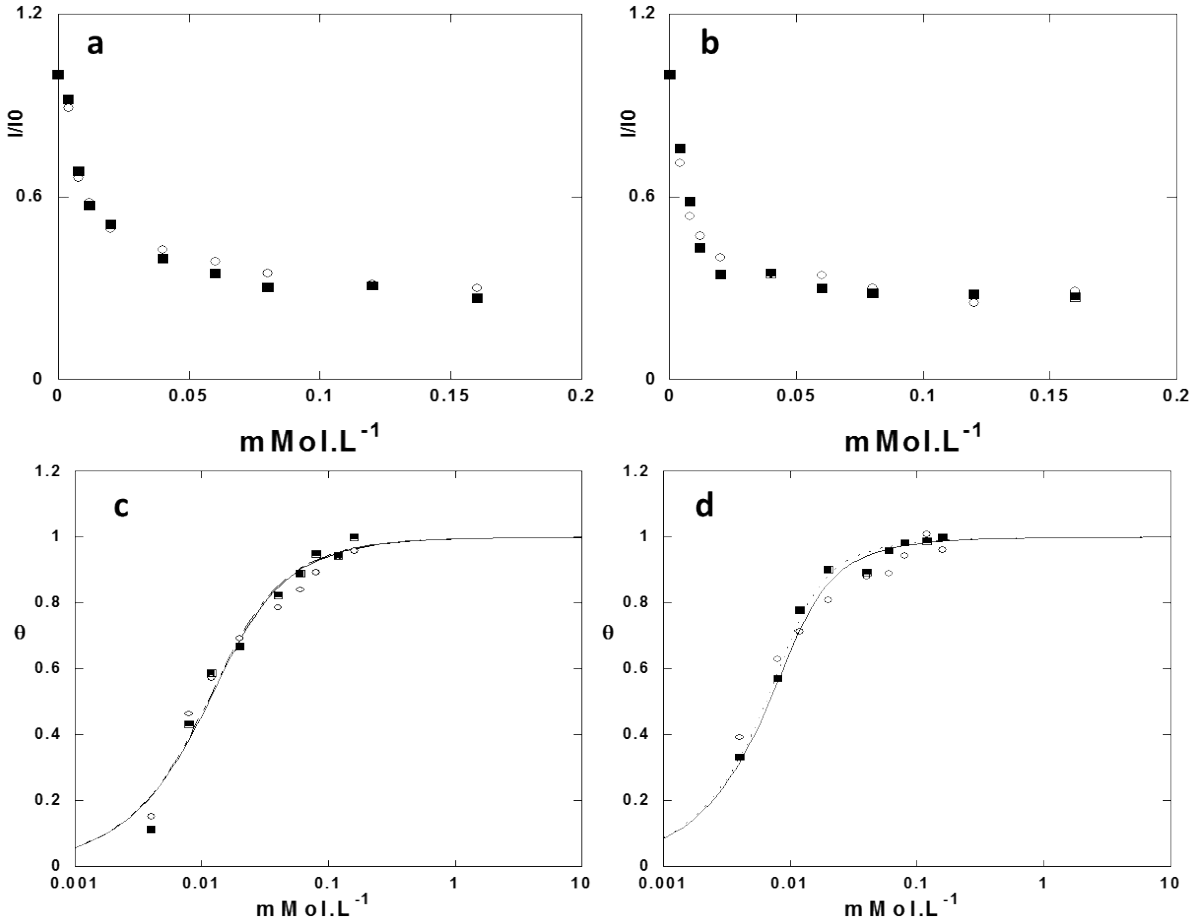

Figure SI5. (a) and (b) Normalized emission of ZnO Ncs in the presence of octanhiol (o) and dodecanthiol (■), (a) isotropic; (b) rods. (c) and (d) Langmuir adsorption isotherm of thiols C8 (o) et C12 (■) and corresponding fit for (c) isotropic and (d) anisotropic ZnO Ncs.

Alkyl-phosphonic acid: The emission intensity of ZnO Ncs decreased upon addition of hexyl phosphonic acid solution in THF (from 4 to 160 µmol.L^{-1}) for both samples (isotropic or anisotropic NPs). However, we observed the formation of a precipitate when the colloidal ZnO Ncs solution contains more than 40 µmol.L^{-1} of hexylphosphonic acid. This observation was noticed in the UV-visible spectra with an increase of the absorption (below 600 nm) upon increasing the concentration of hexylphosphonic acid (Figure SI5). Regarding isotropic ZnO NPs, a plateau was observed when 40 – 60 µmol.L^{-1} of hexyl-phosphonic acid was added with $I/I_0 \approx 26$ %. Anisotropic NPs showed a complete extinction of the emission intensity ($I/I_0 \approx 2$ %) when 40 µmol.L^{-1} of hexyl-phosphonic acid was introduced.

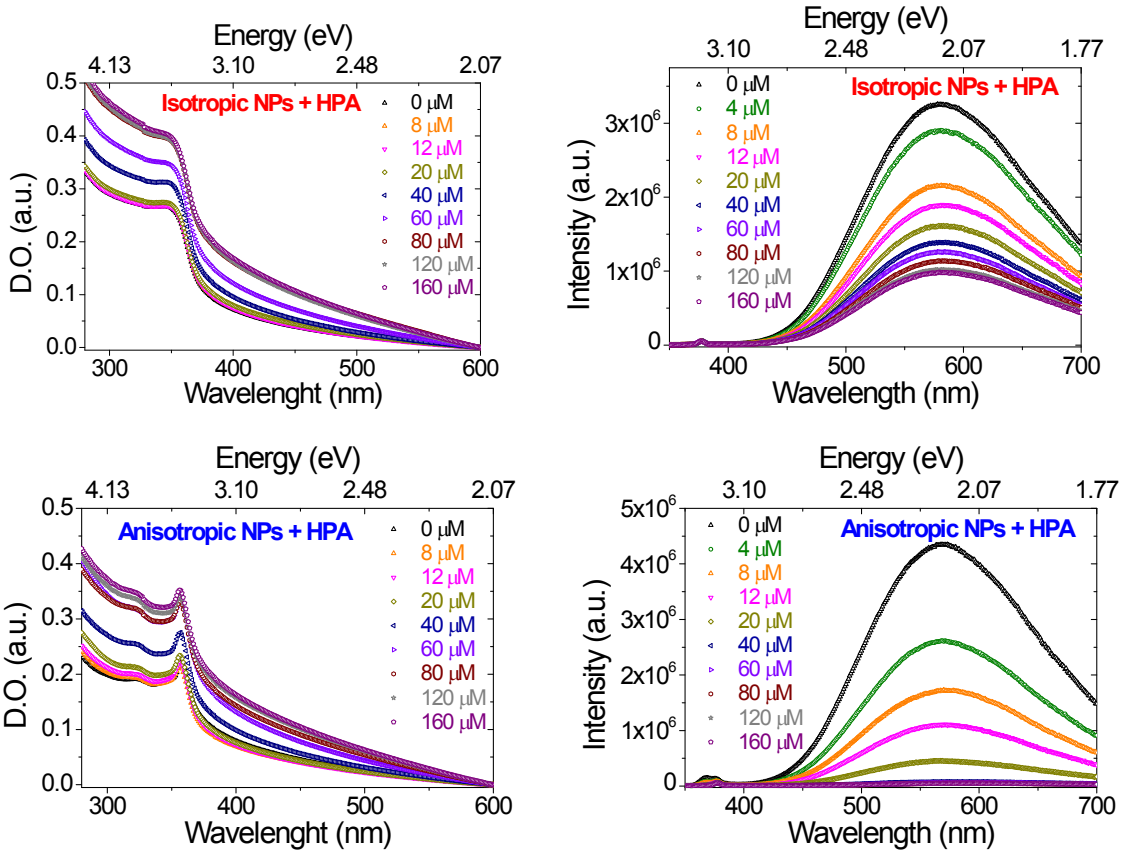

Figure SI6: Absorption and emission spectra of isotropic and anisotropic ZnO NPs in the presence of an increasing amount of hexylphosphonic acid (HPA)

In the case of a longer alkyl phosphonic acid chain: tetradecyl phosphonic acid, TDPA, Figure SI6), a similar precipitate of the colloidal solutions was observed when 40 µmol.L^{-1} was added. The reduction of the emission intensity of the isotropic NPs ZnO solution reached a plateau after addition of 40 µmol.L^{-1} of TDPA with slightly higher $I/I_0 \approx 33$ % in comparison with what was observed in the presence of HPA. Regarding anisotropic NPs ZnO solution, a

similar plateau was reached after the introduction of 40 µmol.L^{-1} of TDPA. As for HPA, we can notice the extinction of the emission intensity with $I/I_0 \approx 5$ %.

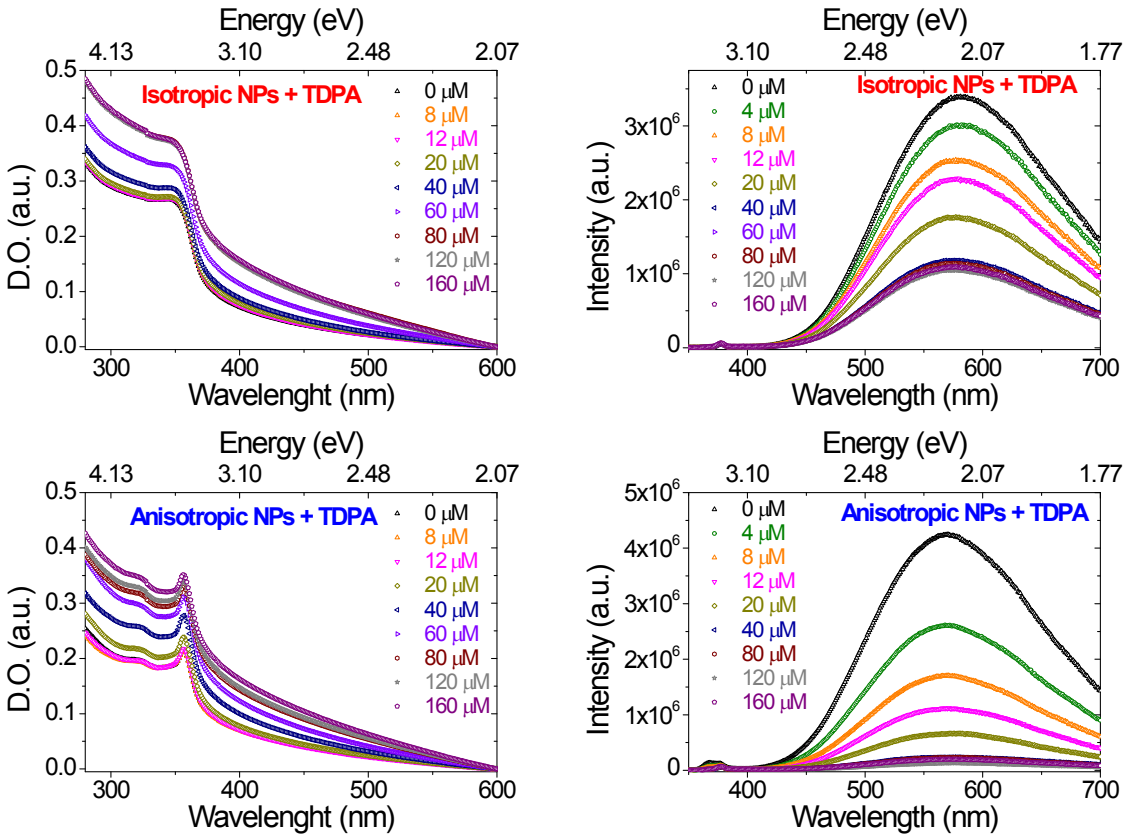

Figure SI7: Absorption and emission spectra of isotropic and anisotropic ZnO NPs in the presence of an increasing amount of tetradecylphosphonic acid (TDPA).

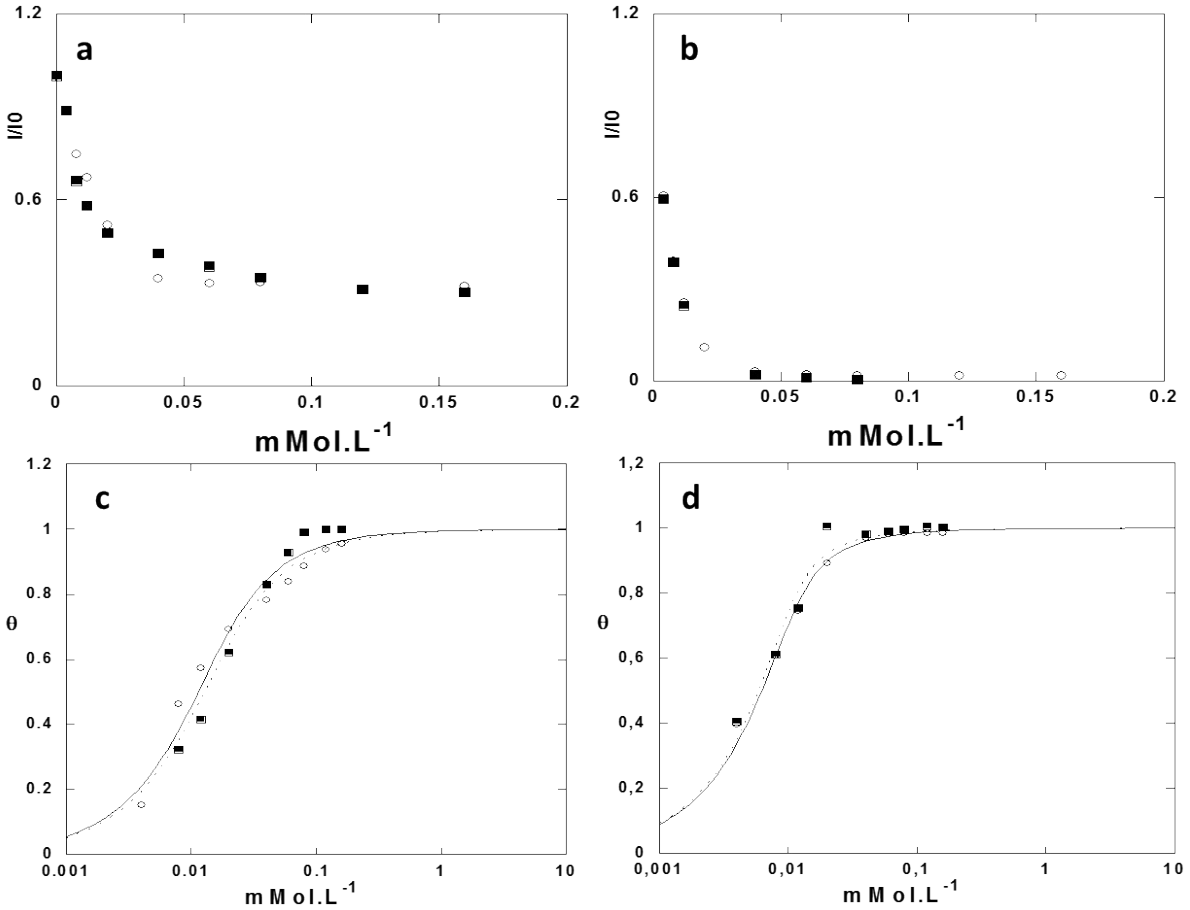

Figure SI8. (a) and (b) Normalized emission of ZnO Ncs in the presence of HPA (o) and HDPA (■), (a) isotropic; (b) rods. (c) and (d) Langmuir adsorption isotherm of thiols C8 (o) et C12 (■) and corresponding fit for (c) isotropic and (d) anisotropic ZnO Ncs.

Alkyl-carboxylic acid: The addition of lauric acid (AL) from 0.4 to 4 mM to a colloidal solution of isotropic ZnO NPs shows no change of the photoluminescence response. However, in the case of anisotropic ZnO NPs solution, a decrease of the emission intensity was noticed when an increase concentration of lauric acid was added (from 0.4 to 4 mM, Figure SI7). Note however that in order to notice a change in the photoluminescence response of anisotropic ZnO NPs, the concentration of AL was at least 100 times higher than the one needed for alkyl-thiol or alkyl-phosphonic acid.

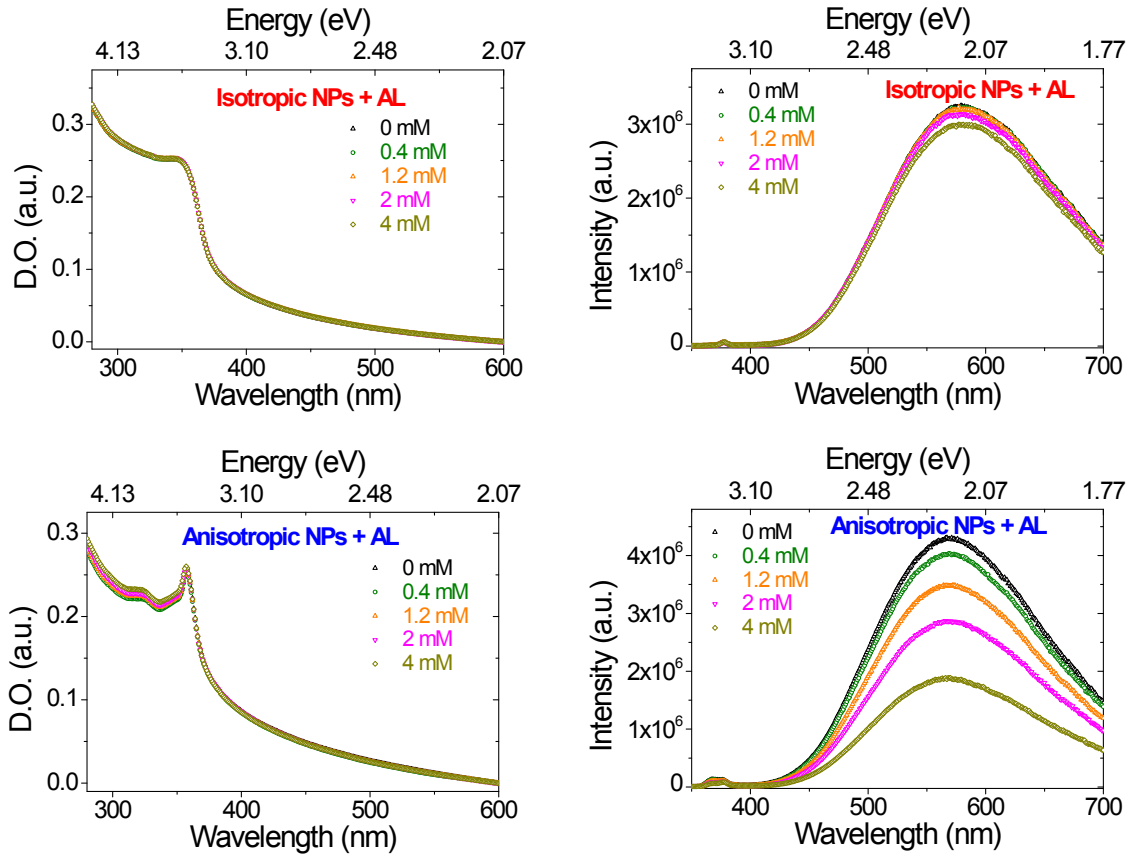

Figure SI9: Absorption and emission spectra of isotropic and anisotropic ZnO NPs in the presence of an increasing amount of lauric acid (AL)

Alkyl-aldehyde: When a solution of hexanal was used, a similar behavior is observed for the photoluminescence properties of both isotropic and anisotropic ZnO NPs solutions than the one observed with lauric acid (Figure SI8). Indeed, no change of photoluminescence response of the colloidal solution of isotropic ZnO NPs was detected upon addition of 4 mM of hexanal while a decrease of the emission intensity of the solution of anisotropic ZnO NPs was noticed after addition of 0.4 to 4 mM of hexanal.

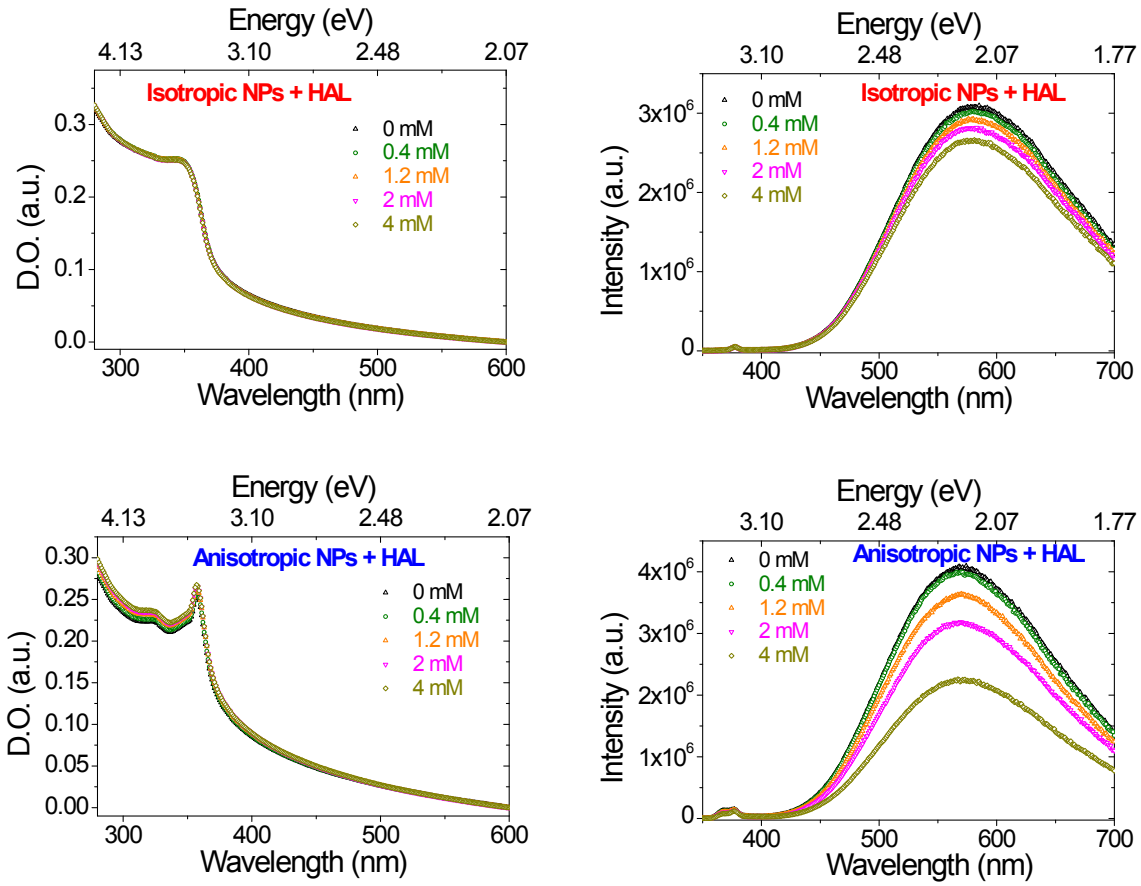

Figure SI10: Absorption and emission spectra of isotropic and anisotropic ZnO NPs in the presence of an increasing amount of hexanal (HAL)

Alkyl-carbonyl and alkyl-alcohol: Unlike the previous organic molecules, the addition of hexan-2-one or octanol did not affect the emission of neither isotropic nor anisotropic NPs even after the addition of excess of substrate with [C] = 4 mM (Figure SI9).

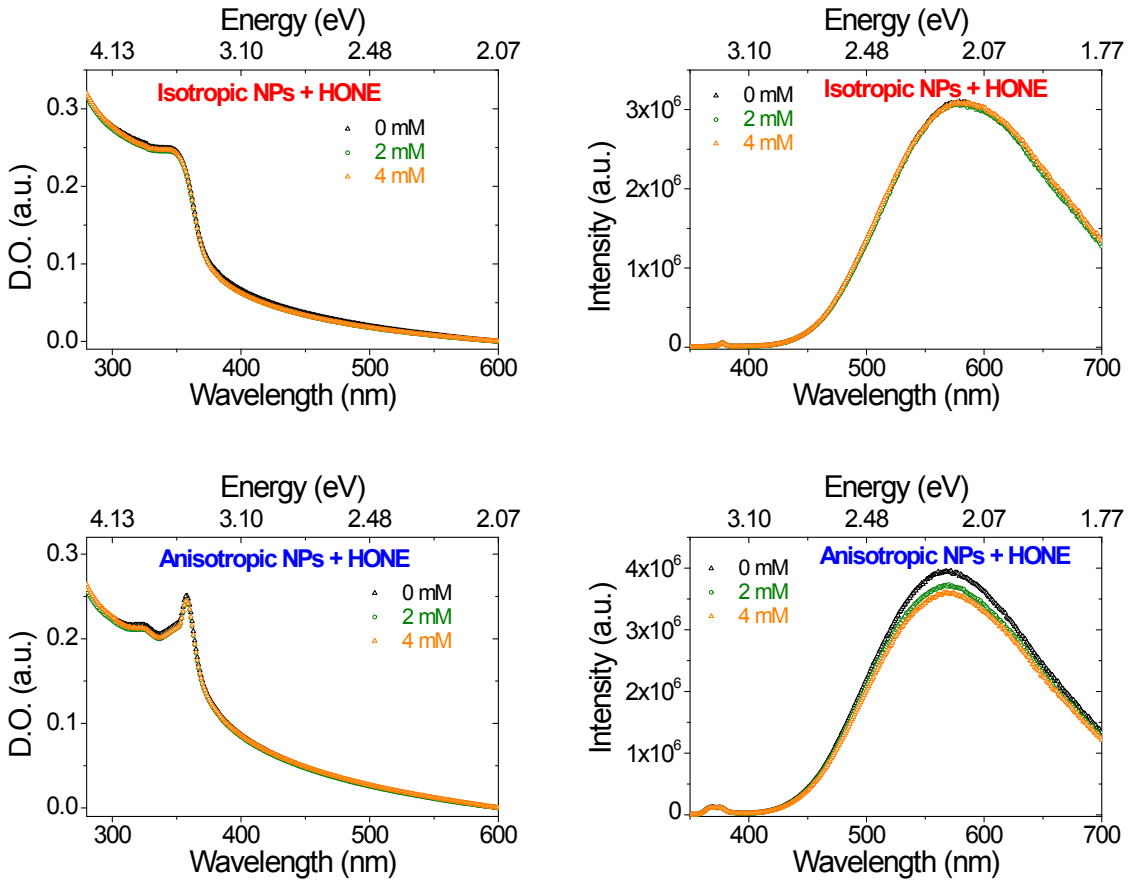

Figure SI11: Absorption and emission spectra of isotropic and anisotropic ZnO NPs in the presence of an increasing amount of hexan-2-one (HONE).

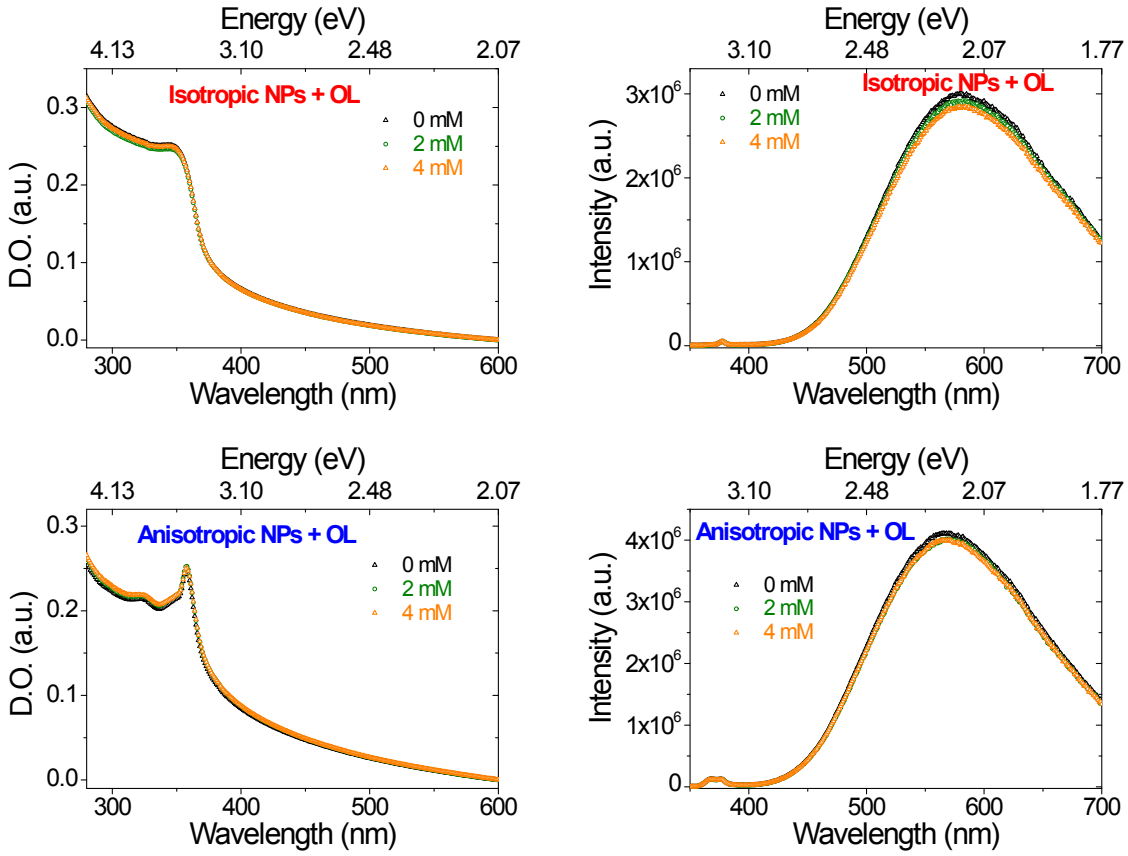

Figure SI12: Absorption and emission spectra of isotropic and anisotropic ZnO NPs in the presence of an increasing amount of octanol (OL)

4. NMR spectroscopic study

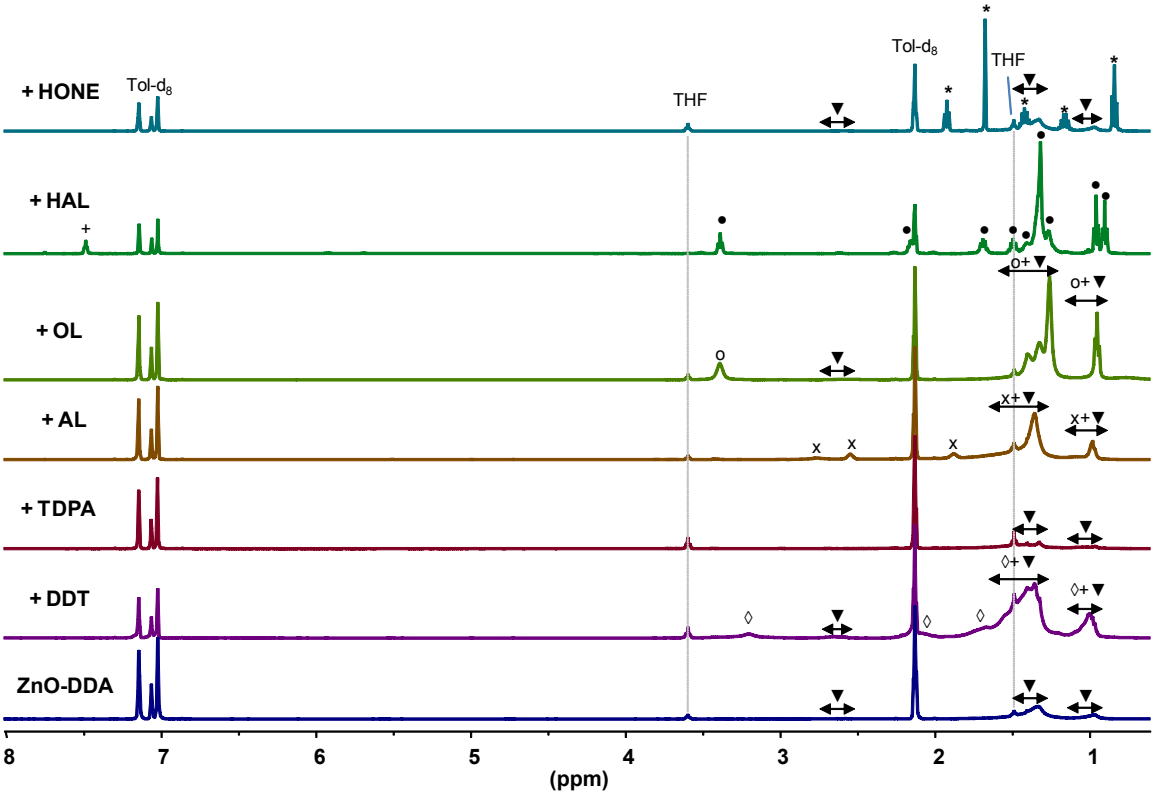

Figure SI13: Full ^{1}H NMR spectra in Tol-d_8 of ZnO stabilized with DDA (ZnO-DDA,▼) and with additional dodecanethiol (DDT, ◊), tetradecylphosphonic acid (TDPA), lauric acid (AL), octanol (OL, o), hexanal (HAL) and hexan-2-one (HONE, *). x and ● indicate the resonances of respectively carboxylate-amonium and imine molecules that appear when carboxylic acid or alkyl-aldehyde are added, respectively.

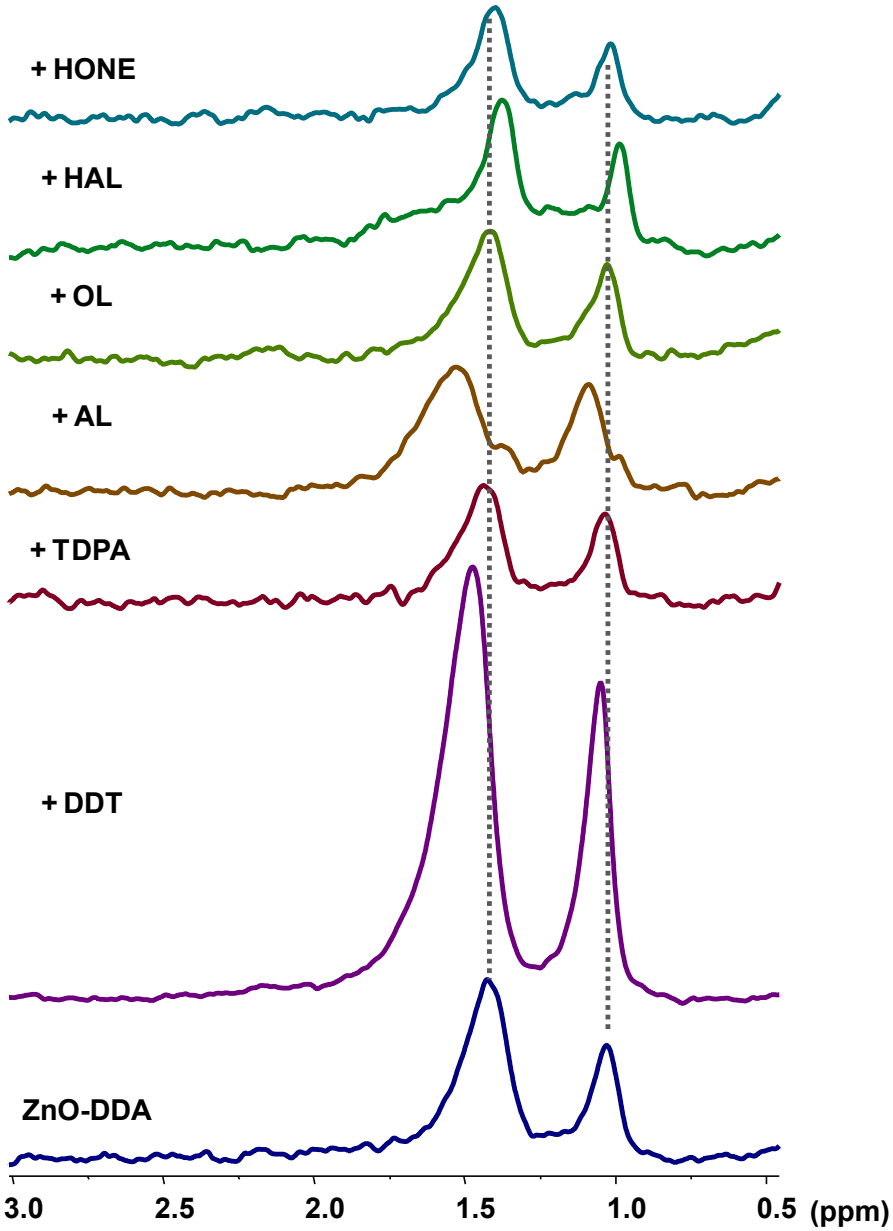

Figure SI14: Diffusion filtered ^{1}H NMR spectrum in Tol-d_8 of ZnO stabilized with 0.2 eq. of DDA and and with additional 0.2 eq. of dodecanethiol (DDT), Tetradecylphosphonic acid (TDPA), Lauric Acid (AL), Octanol (OL), Hexanal (HAL) and Haxan-2-one (HONE). The diffusion filter was set in order to keep the signal of slow diffusing species strongly bound to the ZnO Ncs with $D < 1 \times 10^{-10}$ m^2 s^{-1}.

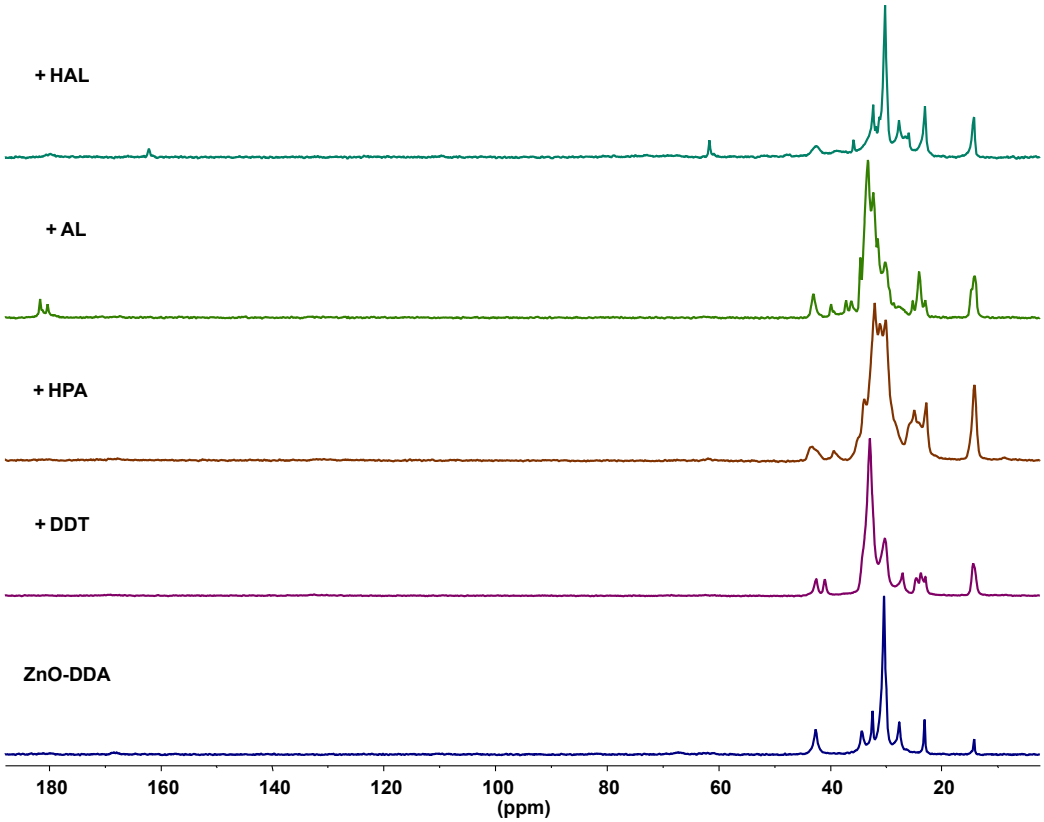

Figure SI15: Full ^{13}C CPMAS NMR spectra of ZnO-DDA and in the presence of Dodecanethiol (DDT), Hexylphosphonic acid (HPA), Lauric Acid (AL) and Hexanal (HAL).

ZnO/alkyl amine: The reference solution, ZnO/DDA, shows mostly broad resonances typical of the alkyl chain in interaction with the ZnO Ncs at 2.57 (α-CH_2), 1.34 (central CH_2) and 0.97 (CH_3) ppm (Figure SI16). Indeed, broadening of the resonance is due to short transverse T_2 relaxation time, which is related mostly to reduced local mobility but can also be due to surface heterogeneity. The DOSY experiment evidences two different kind of DDA molecules (Figure SI17). The first one possess a diffusion coefficient equal to D= (0.7 ± 0.2) × 10^{-10} m^2 s^{-1} characteristic of strongly bonded DDA molecule to ZnO Nc. The second one possess a diffusion coefficient equal to D = (8.3 ± 0.2) × 10^{-10} m^2 s^{-1} corresponding to DDA in weak interaction with the NPs (fast exchange in the NMR timescales). In this case, the percentage of DDA molecules that are free, in weak, or strong interaction with the ZnO Ncs is equal to 15(±5) %, 15(±5) % and 70(±5) %, respectively. The presence of these two different kind of DDA molecules in interaction with the ZnO Ncs is confirmed by filtered ^1H NMR spectra (Figure SI14 ZnO-DDA).

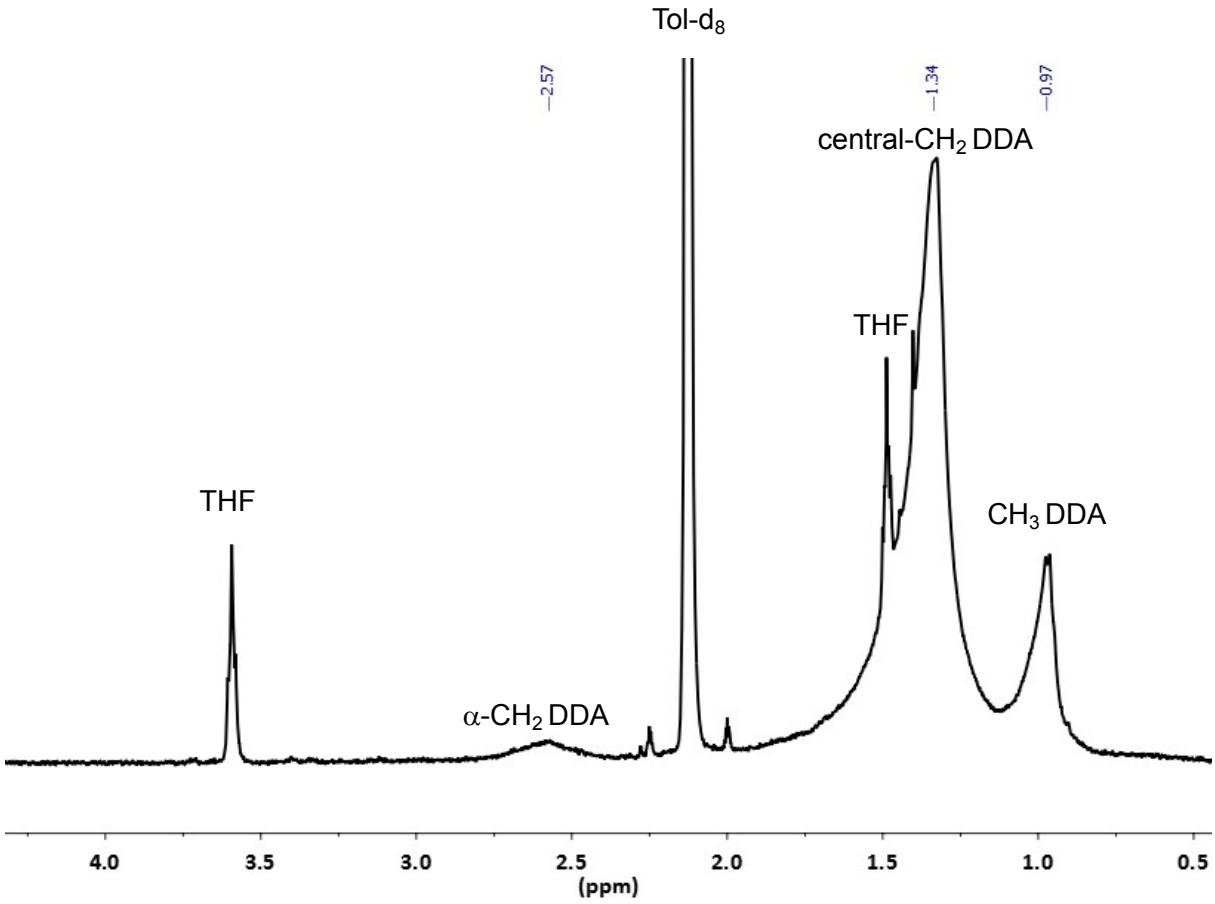

Figure SI16: ^{1}H NMR spectrum in Tol-d_8 of ZnO/DDA.

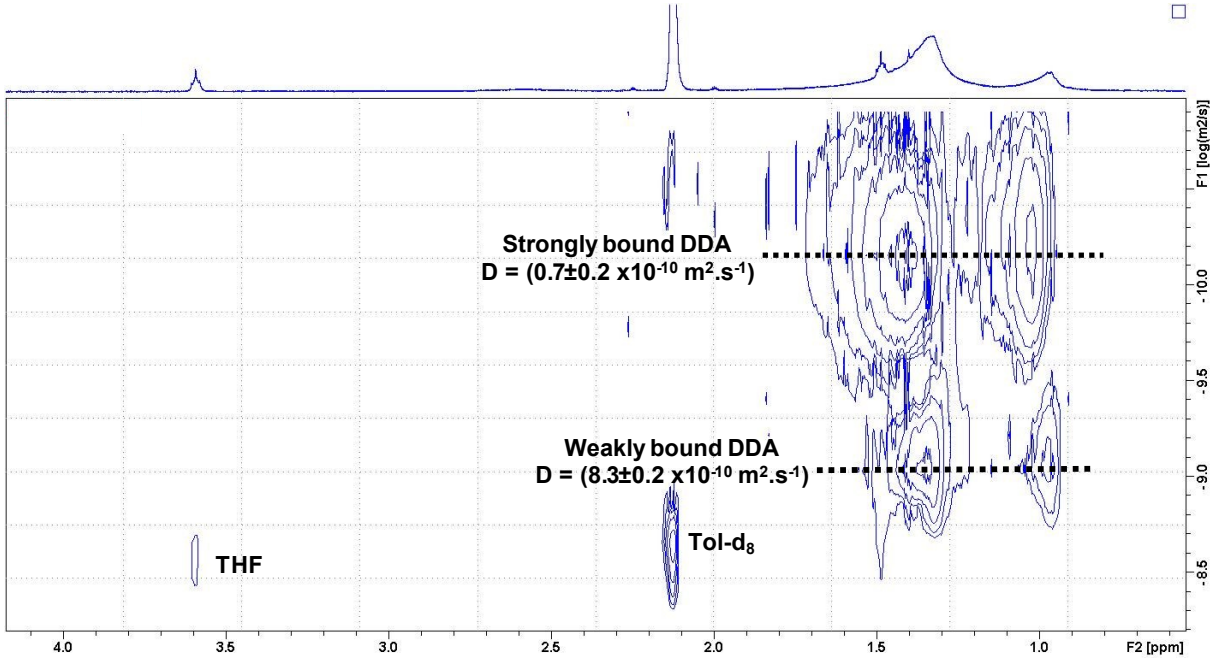

Figure SI17: ^{1}H DOSY NMR spectrum in Tol-d_8 of ZnO/DDA.

Alkyl thiol: When thiol molecules are introduced in the ZnO/DDA colloidal solution, strong modifications are observed in the ^{1}H NMR spectrum: several signals characteristic of new species appear (Figure SI18). First, a small sharp signal at δ = 2.21 ppm associated with a diffusion coefficient equal to D = (10.8 ± 0.4) × 10^{-10} m^2 s^{-1} (Figure SI19) - a values similar to the one measured for pure DDT in toluene (DDT = (11.0 ± 0.2) × 10^{-9} m^2 s^{-1}) - can be attributed to the α-CH_2 protons of the free or very weakly bound thiol ligands (probably in a fast exchange on the NMR timescale). Other new broad DDT signals notably in the 3.5 - 3.0 ppm and 2.2 - 2.0 ppm chemical shift ranges possessing a diffusion coefficient equal to D = (2.5 ± 0.2) × 10^{-10} m^2 s^{-1} can be clearly evidenced with diffusion filtered ^{1}H NMR experiment (Figure SI19). This D values represent an intermediate values between DDT in interaction with ZnO Ncs and DDT molecules free in solution. A ZnO Nc-ligand component with D = (0.7 ± 0.2) × 10^{-10} m^2 s^{-1} is also observed. This latter can be bring to light on the diffusion filter experiment (Figure SI14+DDT). The diffusion filter experiment exhibiting only signals of the alkyl chain at the methyl extremity, it is not possible to identify the nature of the ligand directly bound to the ZnO Ncs. However, diffusion filter experiments performed in the same experimental conditions for both ZnO/DDA and ZnO/DDA/DDT samples show stronger signals for the ZnO/DDA/DDT sample associate to slight shifts of 30 Hz and 10 Hz for the CH_2 and CH_3 signals, respectively. This indicates a chemical or structural modification of the shell of the ligands directly bound to the Ncs. Furthermore, the broad α-CH_2 signal observed at 2.58 ppm for ZnO/DDA splits into two different signals after the addition of the thiol ligands. In this latter case, a sharp triplet signal is observed at 2.58 ppm. Its diffusion coefficient value is equal to D = (10.1 ± 0.4) × 10^{-10} m^2 s^{-1}. This value is typical for DDA molecules free in solution or in very weak interaction with ZnO Ncs. Additionally, a broad signal at 2.64 ppm significantly sharper than the α-CH_2 signal of ZnO/DDA is also present indicating the presence of weakly bound DDA. These results state that part of the DDA molecules in strong or moderate interaction with the ZnO NC is displaced when DDT molecules are added to the colloidal solution. This result is also confirmed with solid state NMR experiments (Figure 4+DDT). ^{13}C CPMAS signals characteristic of ligand bound to the ZnO Ncs are clearly different for ZnO/DDA and ZnO/DDA/DDT samples. The ^{13}C signal in the 40-45 ppm ranges is characteristic of the α-CH_2 group of DDA. Interestingly, only one ^{13}C signal at 42.5 ppm is observed for ZnO/DDA while two ^{13}C signals at 42.9 and 41.4 ppm are observed when DDT molecule are added. Moreover, the presence of strong additional ^{13}C

resonances in the 20-35 ppm range strengthened the presence of DDT molecules. These results confirm that both DDA and DDT molecules are present in the first ligand shell of the ZnO Ncs and that at least part of them interact strongly with the Ncs surface.

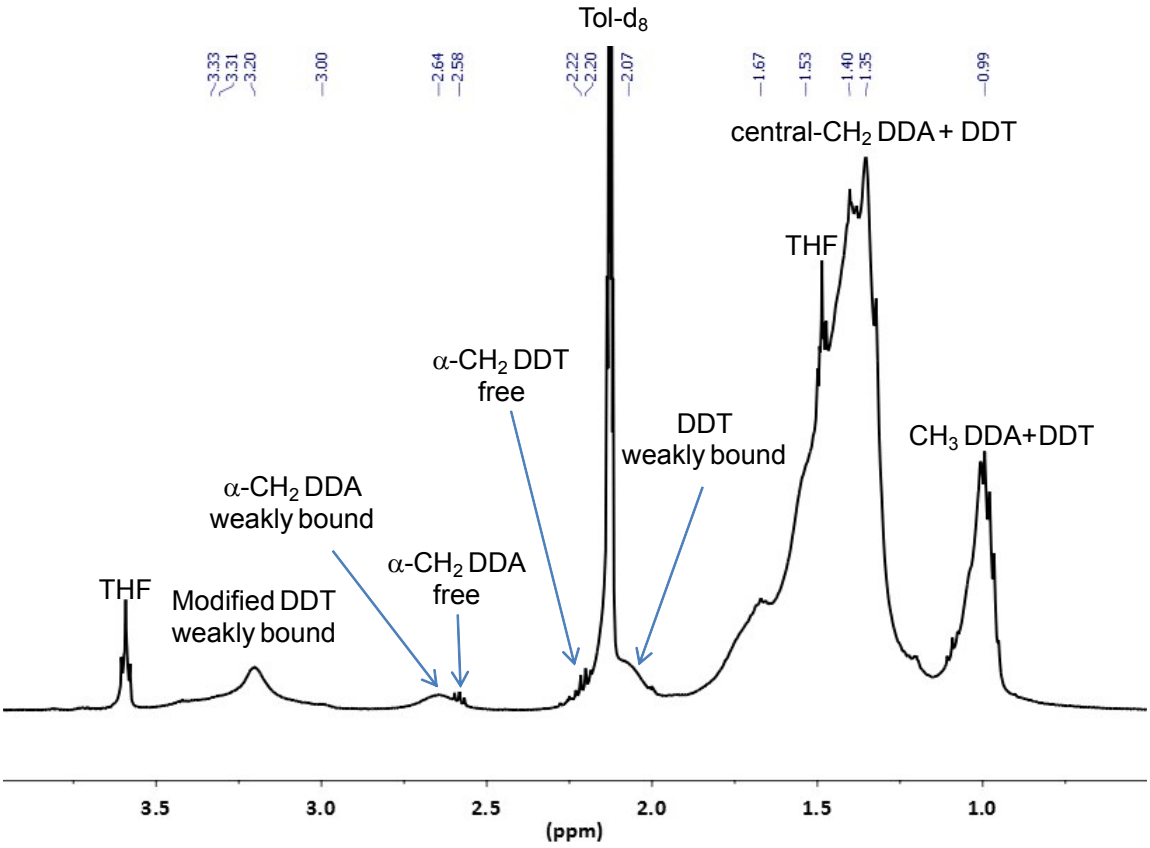

Figure SI18: ^{1}H NMR spectrum in Tol-d_8 of ZnO/DDA after the addition of DDT.

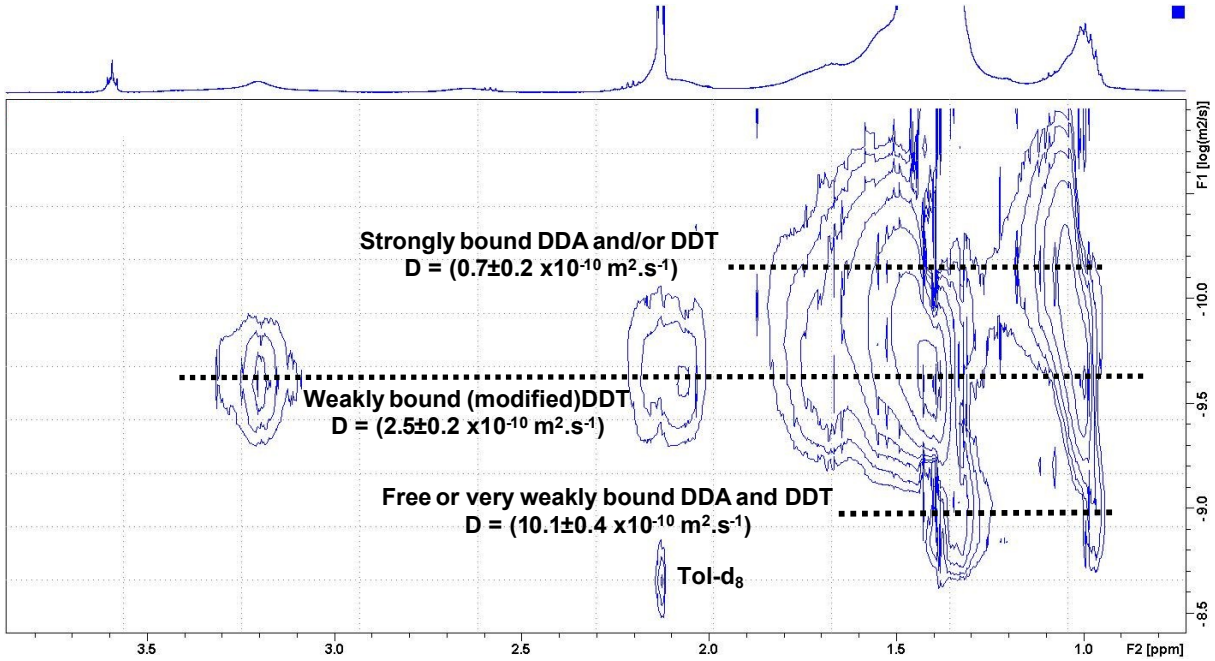

Figure SI19: ^{1}H DOSY NMR spectrum in Tol-d_8 of ZnO/DDA after the addition of DDT.

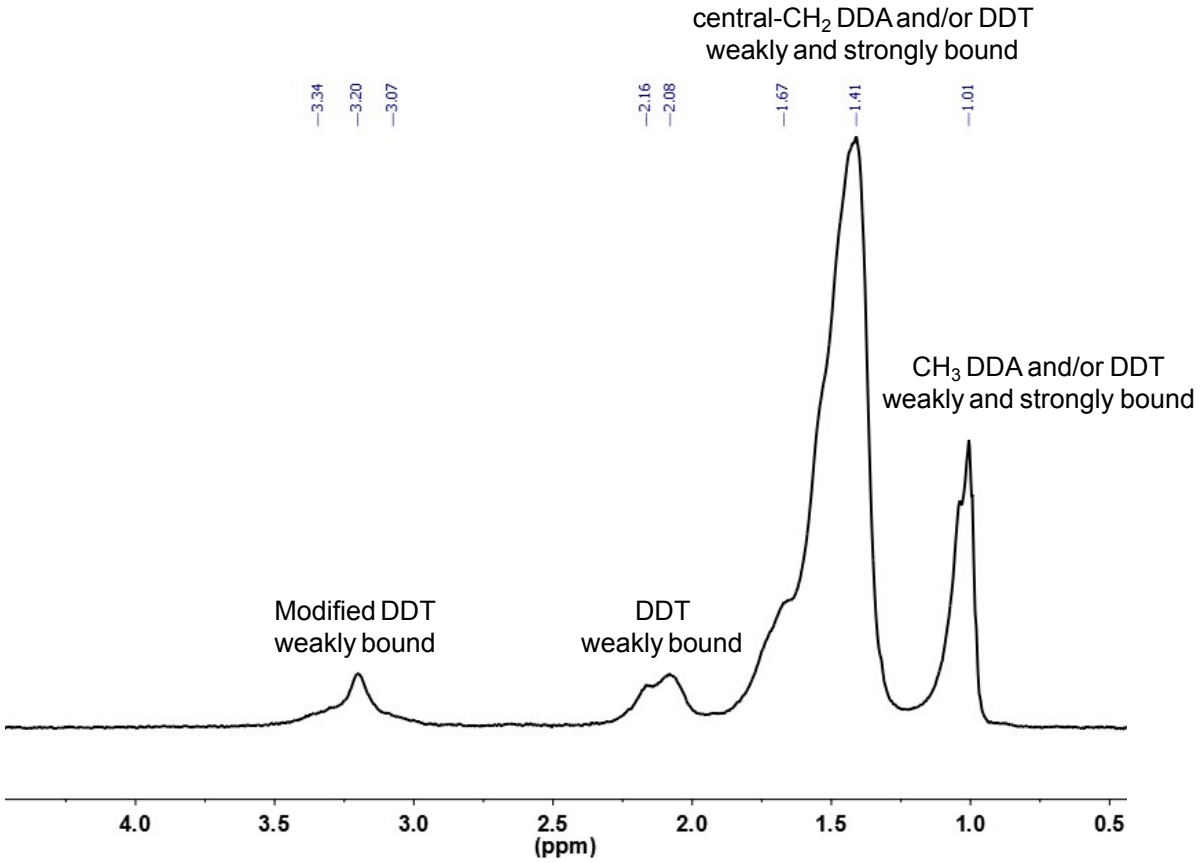

Figure SI20: Diffusion filtered ^{1}H NMR spectrum in Tol-d_8 of ZnO/DDA after the addition of DDT. The diffusion filter was set in order to remove the fast diffusing species (solvent, free or weakly interacting ligands) and to keep the signal of slow diffusing species with $D < 5 \times 10^{-10}$ m^2 s^{-1}.

Alkyl Phosphonic acid:

When phosphonic acid molecules are introduced in the ZnO/DDA colloidal solution, an important precipitation occurs. Liquid NMR spectroscopy has therefore little information. No signals corresponding to phosphonic acid molecules are detected. In addition, a notable decrease of the signal intensity of the peaks associated to ZnO/DDA system is observed (Figure 3+TDPA). DOSY and diffusion filter experiments show that the residual signals are identical to the one of ZnO/DDA system (Figures SI21 and SI14+TDPA, respectively). This indicates that the phosphonic acid molecules associate with ZnO/DDA Ncs and precipitate. Solid state NMR is much more informative in this case. ^{13}C and ^{31}P CPMAS experiments (Figures SI22 and SI23) performed on DDA and phosphonic acid molecules in the absence of ZnO NPs evidence that they form ion-paired species through acid-base reaction. In the absence of ZnO Ncs, ^{13}C signals of DDA and of the hexyl phosphonic acid (HPA) observed in the ^{13}C and ^{31}P CPMAS spectra are displaced when 1 eq. of DDA and of HPA (DDA/HPA) are mixed compare to their position for pure species. Notably the ^{13}C resonance of α-CH_2 DDA shifts from 43.6 ppm for DDA to 39.8 ppm for DDA/HPA. The ^{31}P resonance of the phosphonic acid group shifts from 37.5 ppm for HPA to 21.1 ppm for DDA/HPA due to the deprotonation of phosphonic acid groups. In the presence of the ZnO Ncs, the ^{13}C CPMAS spectra of ZnO/DDA and ZnO/DDA/HPA are clearly different (Figures 4+HPA and SI15+HPA). At least 3 different ^{13}C signals are observed at 43.8, 42.9 and 39.8 ppm in the presence of HPA. The ^{31}P signal of the phosphonic acid group is also very complex. Several resonances are observed between 23.9 and 34.3 ppm (Figure SI23). Undoubtedly, phosphonic acid molecules are present in the first ligand shell of the ZnO Ncs and interact strongly with the Ncs surface.

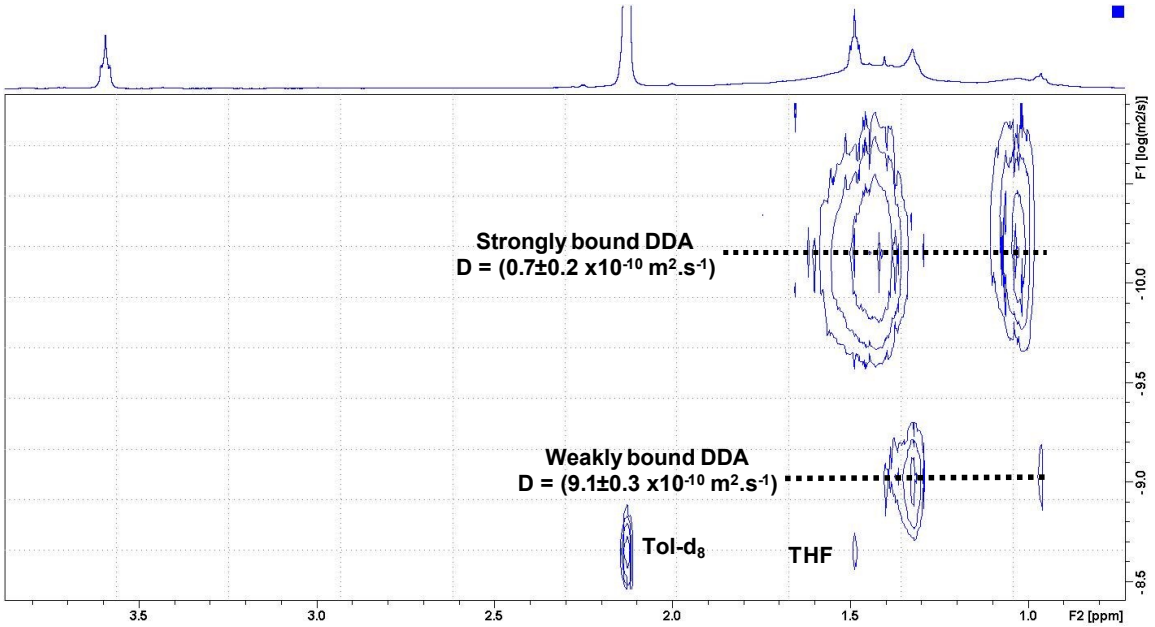

Figure SI21: ^{1}H DOSY NMR spectrum in Tol-d_8 of ZnO/DDA after the addition of TDPA.

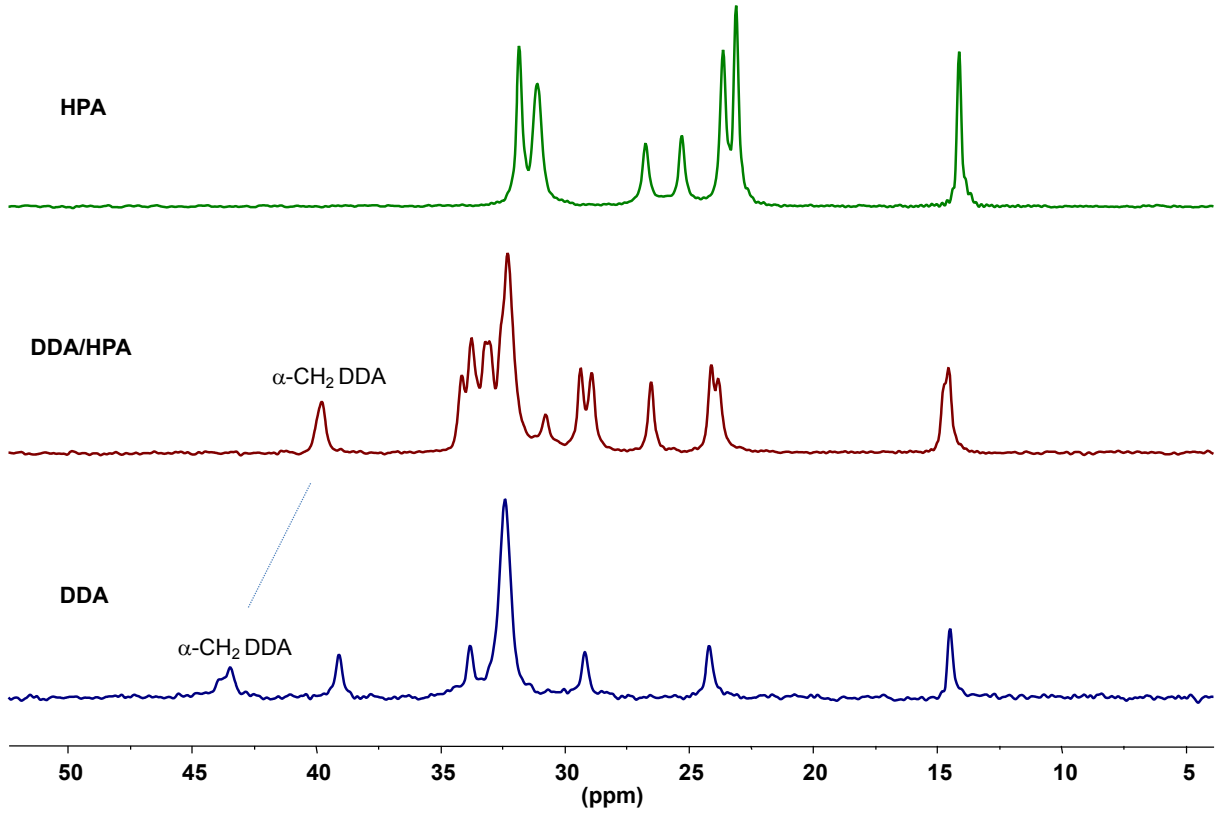

Figure SI22: ^{13}C CPMAS NMR spectra of Dodecylamine (DDA), Hexylphosphonic acid (HPA) and a DDA/HPA 1/1 mixture.

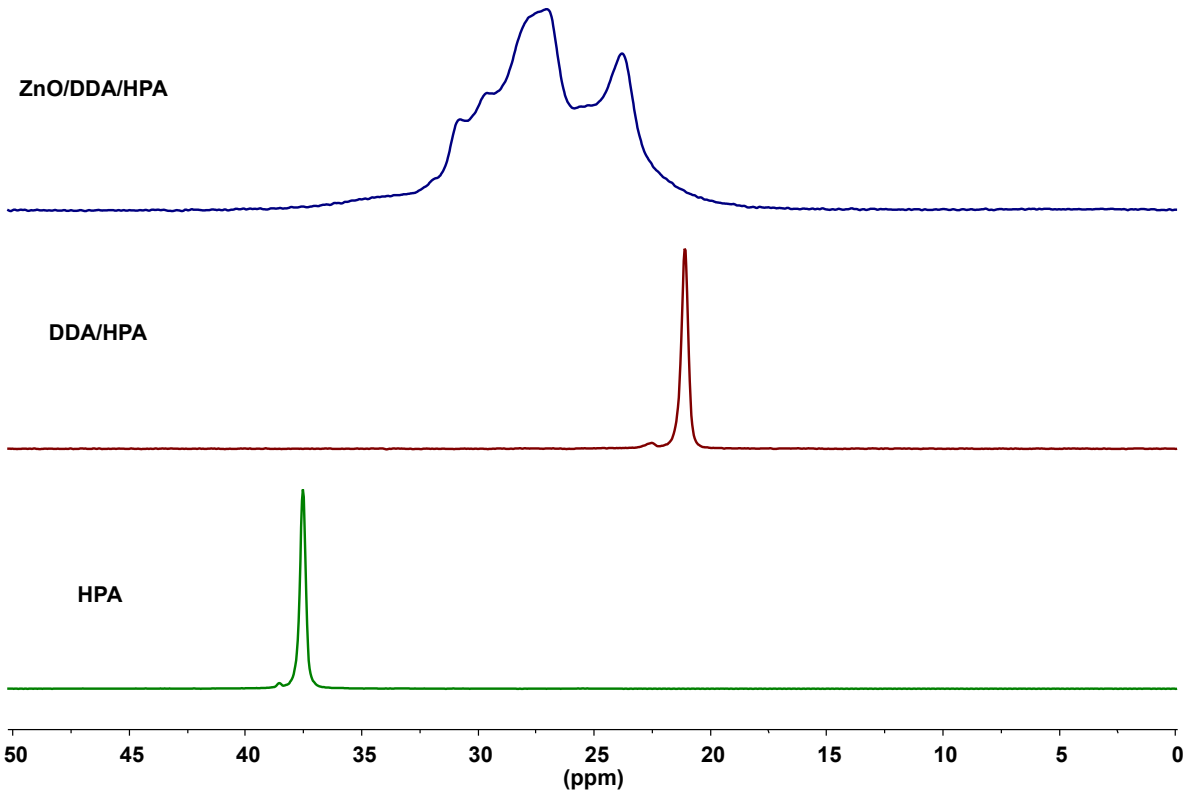

Figure SI23: ^{31}P CPMAS NMR spectra of Hexylphosphonic acid (HPA), a DDA/HPA 1/1 mixture and ZnO/DDA after the addition of HPA (ZnO/DDA/HPA).

Alkyl-carboxylic acid:

When carboxylic acid molecules are introduced in the ZnO/DDA colloidal solution, the formation of carboxylate ammonium ion-pairs in interaction with the ZnO Ncs is observed, as previously reported.[4] The resonance associated to the α-CH_2 of DDA shifts from 2.58 ppm to 2.76 ppm after the addition of lauric acid (Figures 3+AL). The resonances for the α- and β- positions of the carboxylate species are observed at 2.54 and 1.88 ppm. The ion-pairs show a diffusion coefficient of $D = (3.6 \pm 0.2) \times 10^{-10}$ m^2 s^{-1} indicating a weak or moderate interaction with the ZnO Ncs (Figure SI24). A ZnO Nc-ligand component with $D= (0.8 \pm 0.1) \times 10^{-10}$ m^2 s^{-1} is also observed. This latter ZnO-ligand interaction can be bring to light on the diffusion filter experiment (Figure SI14+AL). As for thiol substrates, only signals of the alkyl chain at the methyl extremity can be observed with this experiment, it is therefore not possible to identify the nature of the ligand directly bound to the ZnO NC. However, the diffusion filter experiments performed under the same experimental conditions for both ZnO/DDA and ZnO/DDA/Lauric Acid samples show signals of similar intensities. Only a slight broadening and shifting (50 Hz and 30 Hz for the CH_2 and CH_3 signals, respectively) is

observed in the presence of the carboxylic acid. This indicates a structural or chemical modification of the shell of ligands directly bound to the Ncs. This result is confirmed by solid state ^{13}C CPMAS NMR experiments (Figure 4+AL). Signals characteristic of ligand bounded to the ZnO Ncs are different for the ZnO/DDA and ZnO/DDA/Lauric Acid samples. The α-CH_2 ^{13}C signal of DDA observed at 42.5 ppm for ZnO/DDA slightly shifts to 43.4 ppm when Lauric Acid is present in the colloidal solution. In addition, resonances characteristic of carbonyl group and α-CH_2 group of Lauric Acid molecules are observed respectively at 182.0 and 180.6 ppm and between 36.6 and 40.3 ppm. These results confirm that both Lauric acid and DDA molecules are present in the first ligand shell of the ZnO Ncs and interact with the Ncs surface as ammonium-carboxylate ion pairs.

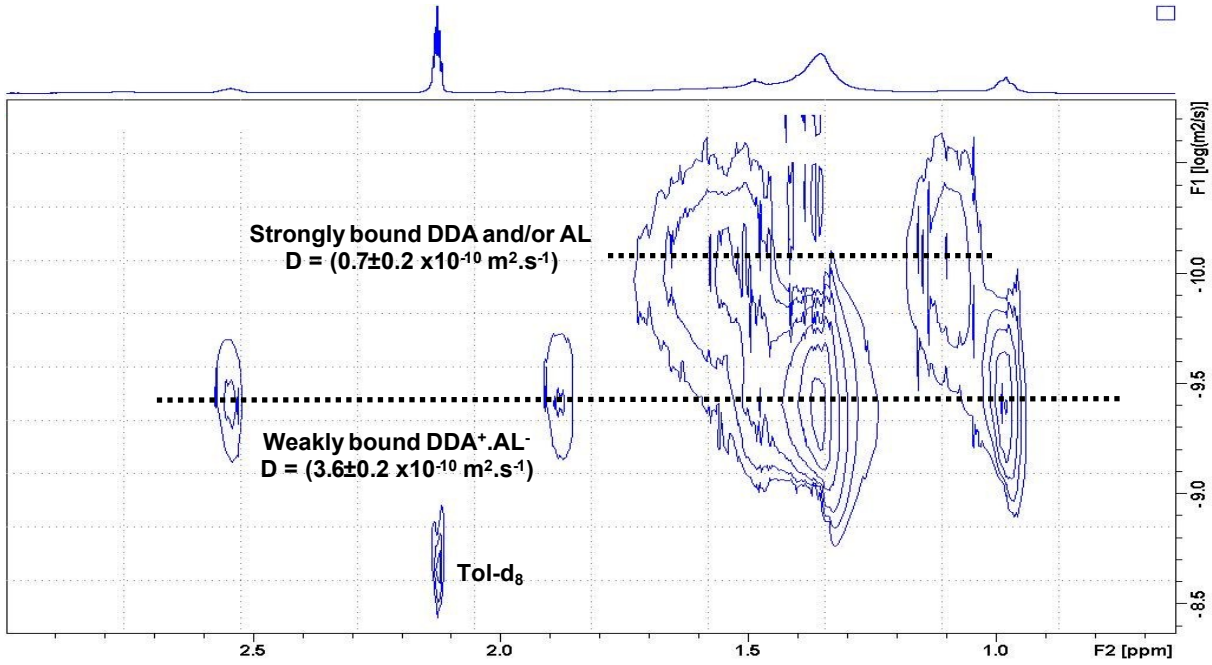

Figure SI24: ^{1}H DOSY NMR spectrum in Tol-d_8 of ZnO/DDA after the addition of AL.

Alkyl-alcohol:

When alkyl alcohol molecules are introduced in the ZnO/DDA colloidal solution, ^{1}H signals characteristic of the octanol molecules are observed (at 3.38, 1.40, 1.32, 1.26 and 0.95 ppm, Figures 3+OL). The broad ^{1}H signal of the α-CH_2 of DDA is not modified (the other DDA signals overlap with the octanol ones). DOSY measurement evidences the presence of ligand strongly bound to ZnO Ncs (D= (0.7 ± 0.2) × 10^{-10} m^2

s^{-1}, Figure SI25) and the diffusion filter spectra (Figure SI14+OL) show that the alkyl chain signals of the strongly bound ligand are not modified by the addition of the octanol molecules. The diffusion coefficient of octanol molecules is equal to D= (14.8 ± 0.4) × 10^{-10} m^2 s^{-1}, a values corresponding to free octanol molecules. However, strong negative NOEs are observed for the fast diffusing octanol molecules (Figure SI26). As previously reported, these negative NOE signals are transfer NOE (trNOE) associated to the fast exchange between octanol molecules in the second ligand shell surrounding the Ncs and octanol free in solution. In conclusion, these results evidence that the first shell of ligand is composed of DDA molecules and that octanol molecules interact only with the ZnO Ncs through the second ligand shell.

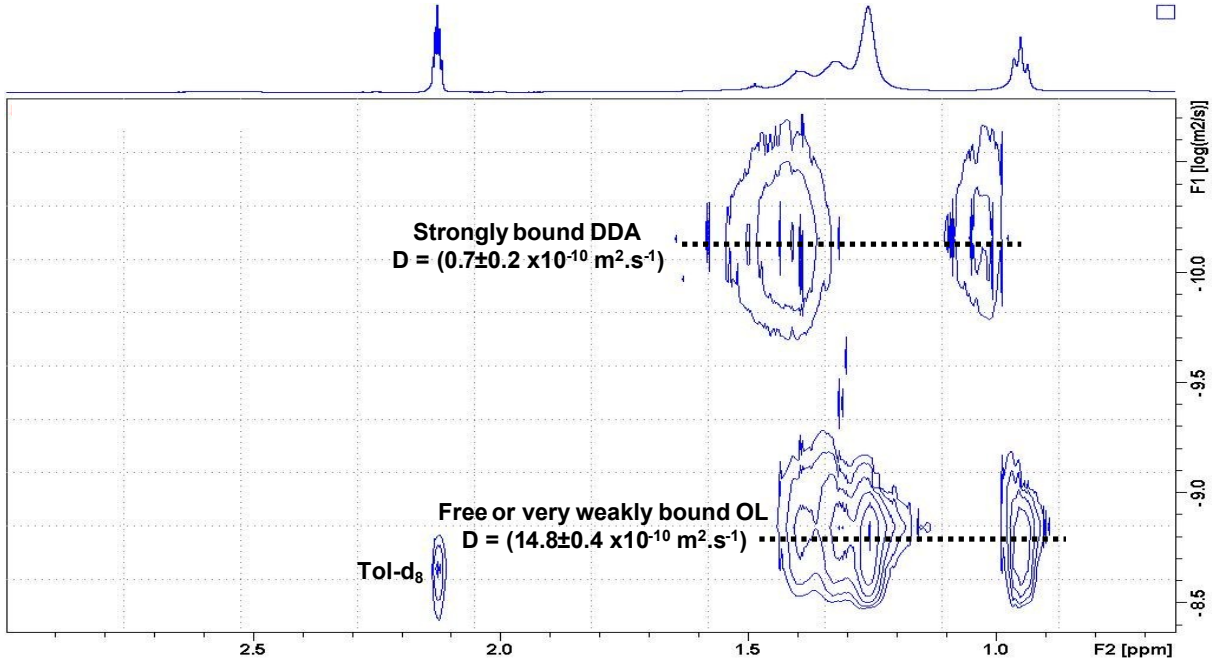

Figure SI25: ^{1}H DOSY NMR spectrum in Tol-d_8 of ZnO/DDA after the addition of OL.

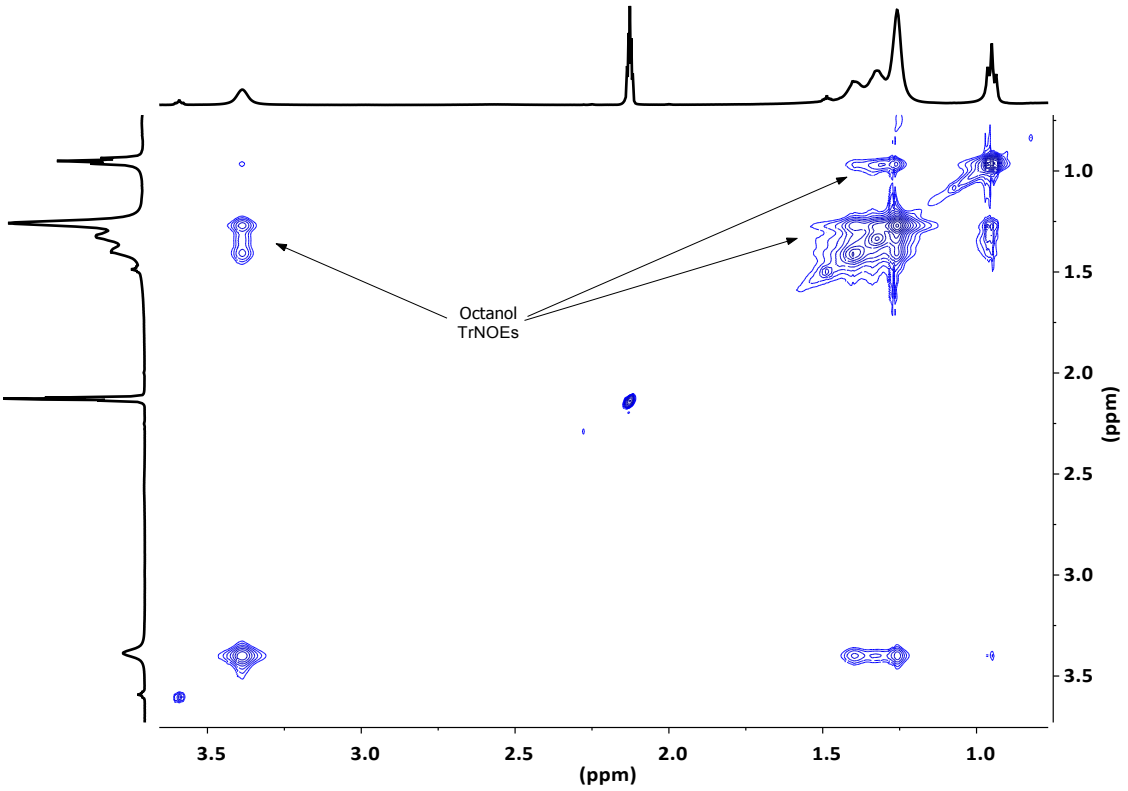

Figure SI26: ^{1}H NOESY NMR spectrum (mixing time 100 ms) in Tol-d_8 of of ZnO/DDA after the addition of OL.

Alkyl-aldehyde: Imine molecules were identified through ^{1}H and ^{13}C signals assignment based on chemical shifts, spin-spin coupling constants, splitting patterns, signal intensities, and by using ^{1}H-^{1}H TOCSY, ^{1}H-^{13}C HMQC and ^{1}H-^{13}C HMBC experiments (Figure SI27). Characteristic imine NMR resonances are the ones of the **CH**=N- (δ^{1}H 7.48 ppm (t) and δ^{13}C 162.5 ppm), =N-**CH_2**- (δ^{1}H 3.38 ppm (t) and δ^{13}C 61.6 ppm), -**CH_2**-CH=N- (δ^{1}H 2.15 ppm (q) and δ^{13}C 35.7 ppm) and =N-**CH_2-CH_2**- (δ^{1}H 1.69 ppm (q) and δ^{13}C 31.3 ppm) groups. DOSY measurement evidences the presence of slow diffusing species with a diffusion coefficient equal to D= (2.8 ± 0.4) × 10^{-10} m^2 s^{-1} (Figure SI28), a value higher than the one measured for ZnO NPs (D= (0.7 ± 0.2) × 10^{-10} m^2 s^{-1}), that correspond to species in weak interaction mode with ZnO Ncs probably through hydrogen bonds. Diffusion filter spectra (Figure SI14+HAL) show that the corresponding alkyl chain signals of these weakly interacting species, are sharper than the ones associated to the strongly bounded DDA molecules in ZnO/DDA. Their chemical shifts are also slightly different from the strongly bounded DDA ones (shifts of -18 Hz and -23 Hz for respectively the CH_2 and CH_3 signals). Additional very broad signals underneath the CH_2 and CH_3 signals are also detected that should correspond to the strongly bound DDA. Their intensities are too weak to measure their diffusion coefficient in the DOSY experiment. A diffusion coefficient at D= (9.7 ± 0.3) × 10–

^{10} m^2 s^{-1} is measured for the imine resonances and is similar to the diffusion coefficient of the free imine molecules. However, trNOEs signal are observed in the ^{1}H NOESY NMR spectrum, stating that these imine molecules are in weak interaction with ZnO Ncs (Figure SI29). Solid state experiments confirm these results (Figures 4+HAL and SI15). The ^{13}C CPMAS spectrum exhibits sharp resonances characteristic of imine species as well as resonances associated to DDA. The ^{13}C signal associated to α-CH_2 of DDA is observed at 42.5 ppm (as for ZnO/DDA system) but the signal is notably broader in the presence of hexanal. In addition, the resonance associated to β-CH_2 of DDA shifts from 34.5 to 33.0 ppm. A broad resonance that could correspond to α- or β-CH_2 groups of DDA in different environment is also observed at 39.0 ppm. The sharpness of characteristic imine resonances (at 161.9, 61.4 and 35.7 ppm) suggests a high mobility of the imine molecules. This result is confirmed by the strong increase of the intensity of theses resonances (compare to the DDA resonances) when ^{13}C direct polarisation MAS experiment are performed (Figure SI30). These results indicate that the first ligand shell is composed of DDA molecules and that the imine molecules generated *in situ* interact only with the ZnO Ncs through the second ligand shell.

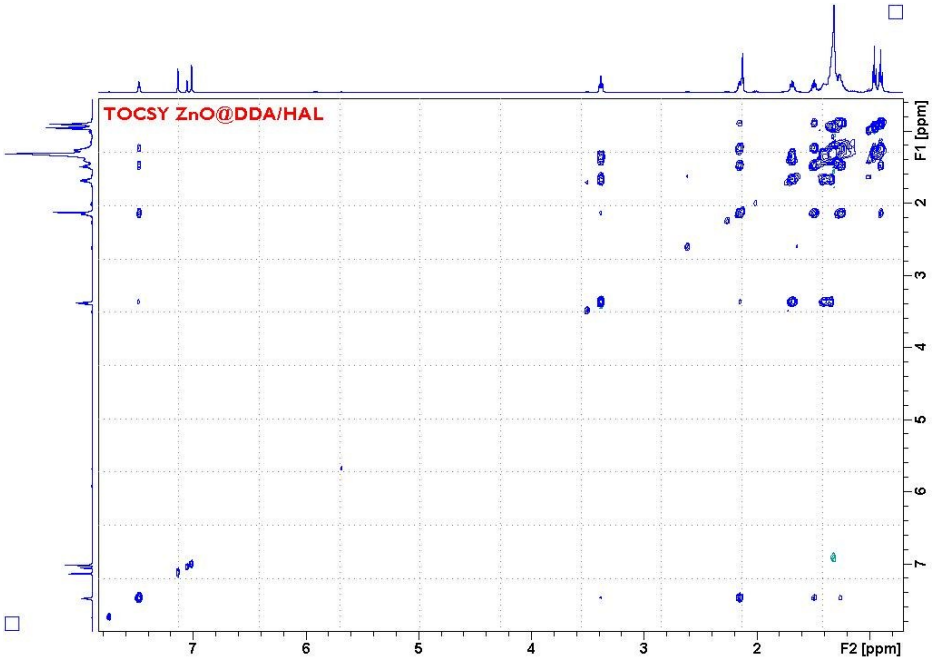

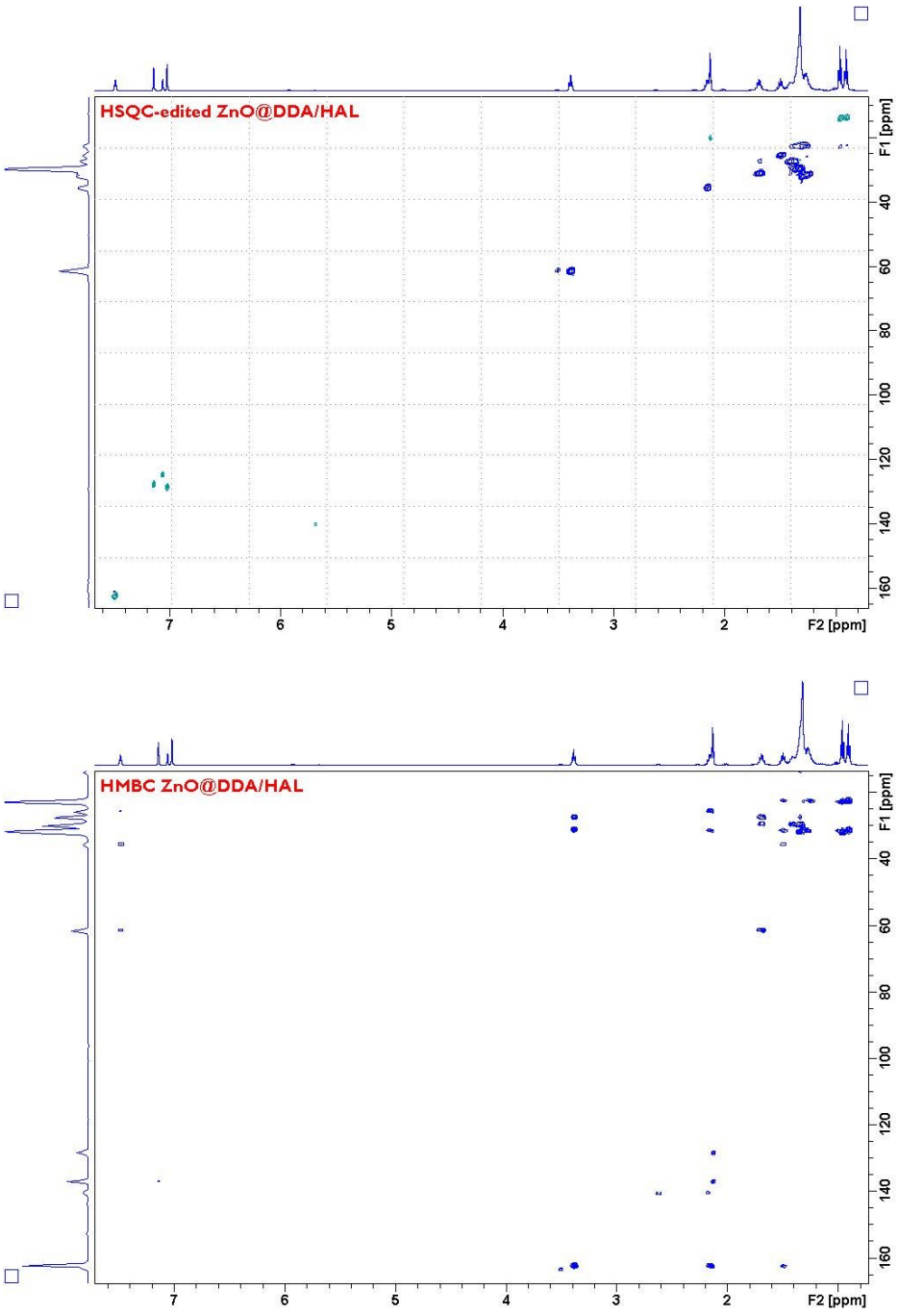

Figure SI27: ^{1}H-^{1}H TOCSY (top), ^{1}H-^{13}C HSQC-edited (middle) and ^{1}H-^{13}C HMBC (bottom) spectra of ZnO/DDA after the addition of HAL in Tol-d_8.

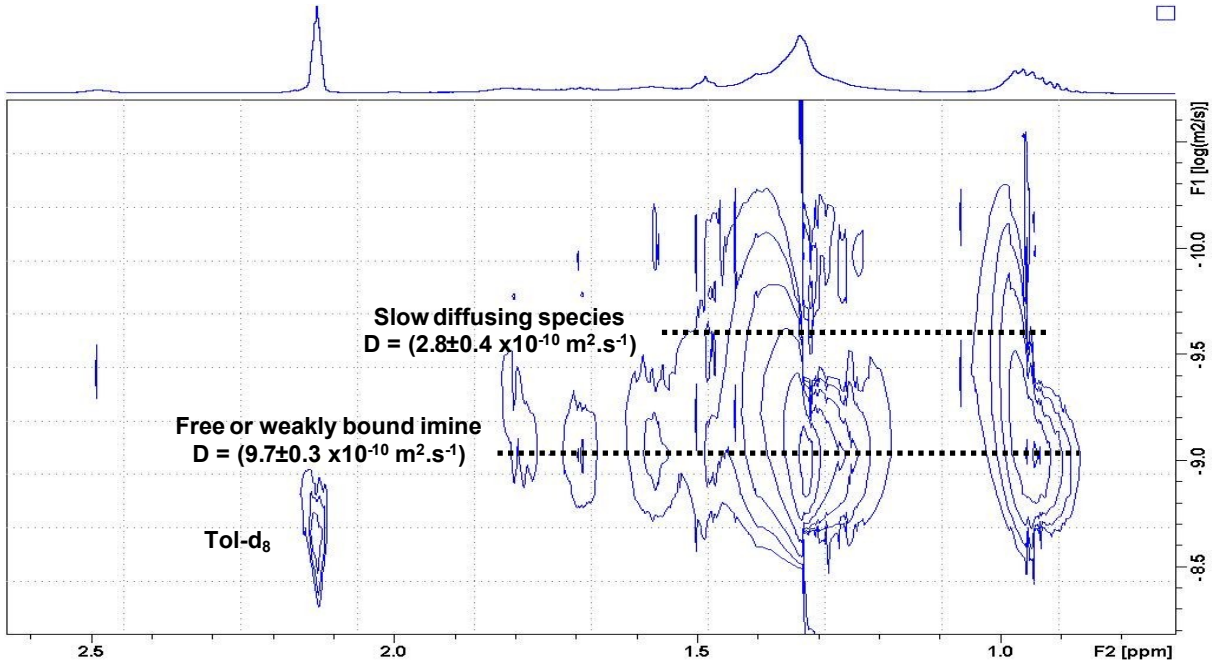

Figure SI28: ^{1}H DOSY NMR spectrum in Tol-d_8 of ZnO/DDA after the addition of HAL.

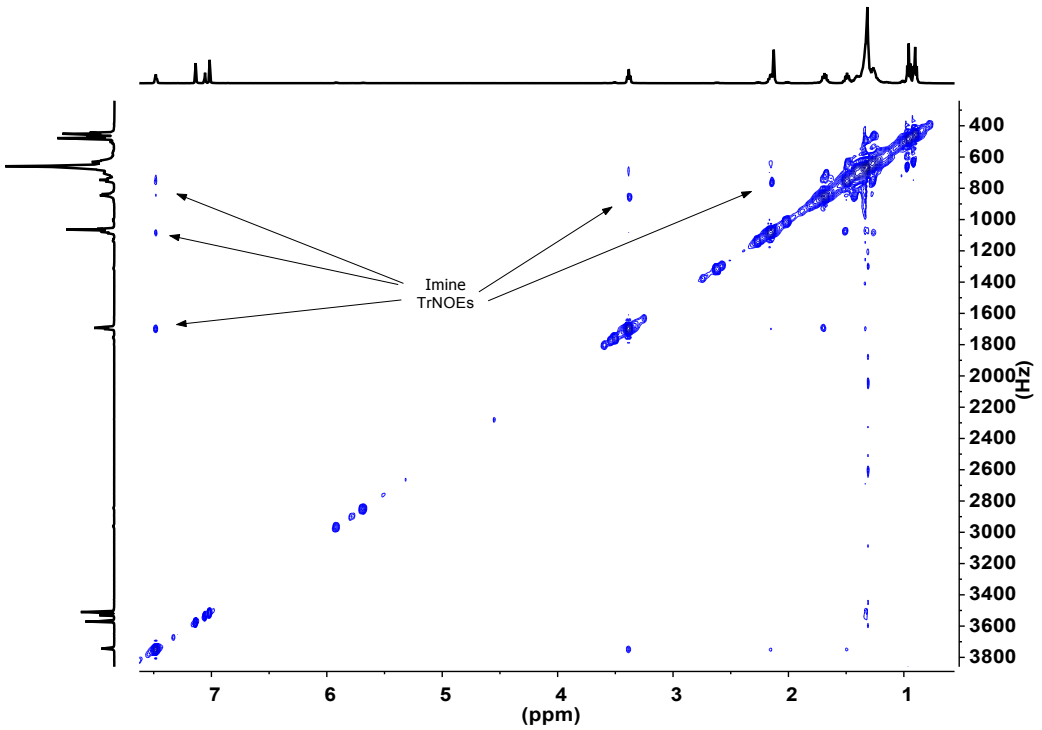

Figure SI29: ^{1}H NOESY NMR spectrum (mixing time 100 ms) in Tol-d_8 of of ZnO/DDA after the addition of HAL.

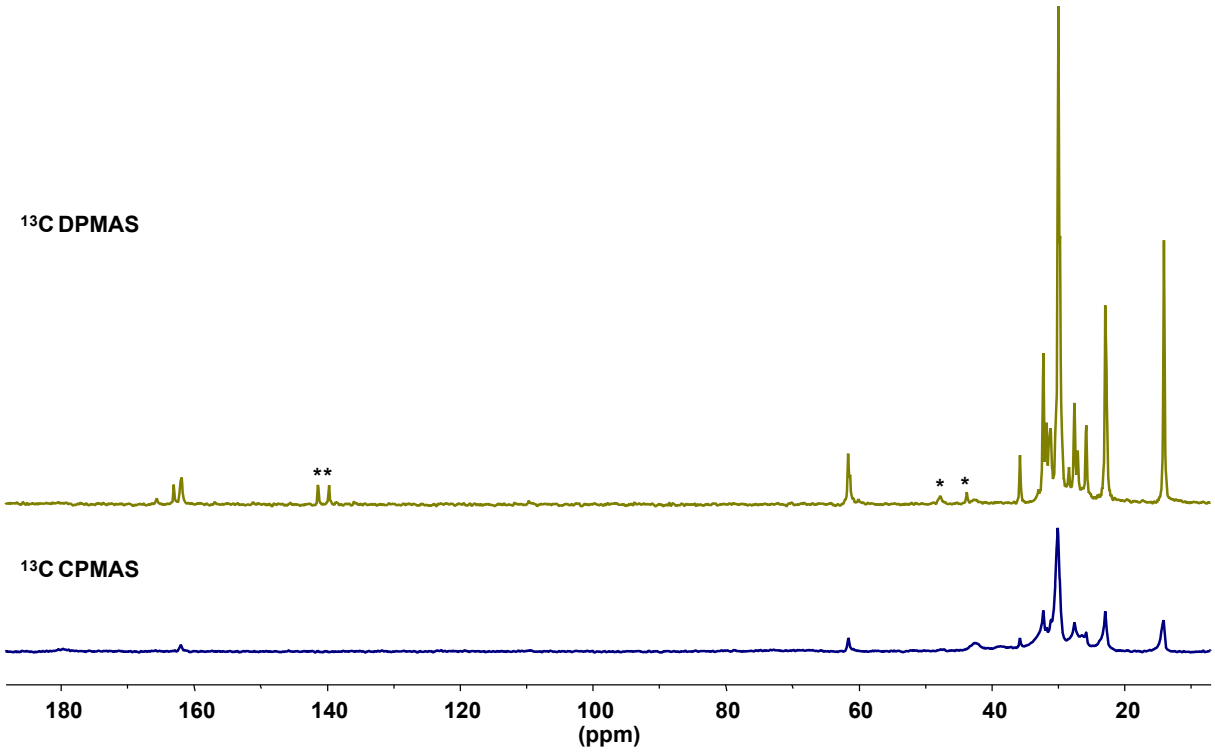

Figure SI30: ^{13}C MAS NMR spectra with cross-polarisation (CP) or direct-polarization (DP) of ZnO / DDA after the addition of HAL. * non identified secondary products with high mobility (not in interaction with the ZnO NCs).

Alkyl-ketone:

When alkyl-ketone (*i.e.* hexanone, HONE) molecules are introduced in the ZnO/DDA colloidal solution, the ^{1}H signals characteristic of the hexanone molecules are observed (at 1.92, 1.68, 1.42, 1.16 and 0.84 ppm, Figure SI5+HONE). In addition, the ^{1}H DDA signals are not modified. DOSY measurement (Figure SI31) as well as the diffusion filter spectra (Figure SI14+HONE) evidence that the alkyl chain signal of the strongly bound ligand is not modified by the addition of the hexanone molecules. The diffusion coefficient of the hexanone molecules present in the ZnO/DDA colloidal solution, D= $(19.6 \pm 0.4) \times 10^{-10}$ m^2 s^{-1}, corresponds to the one measured for free hexanone molecules and no trNOE signal is detected (Figure SI32). These results allow to conclude that alkyl-ketone molecules do not interact at all with ZnO Ncs and do not react with the DDA to form an imine as seen for alkyl-aldehyde (see above).

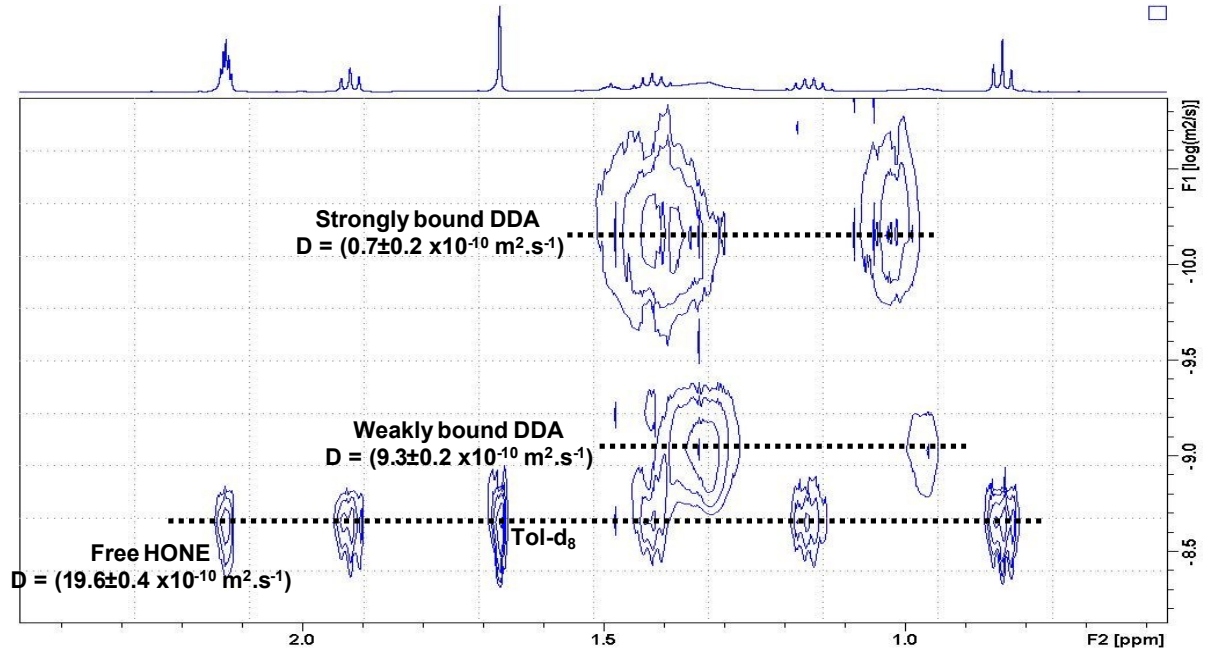

Figure SI31: ^{1}H DOSY NMR spectrum in Tol-d_8 of ZnO/DDA after the addition of HONE.

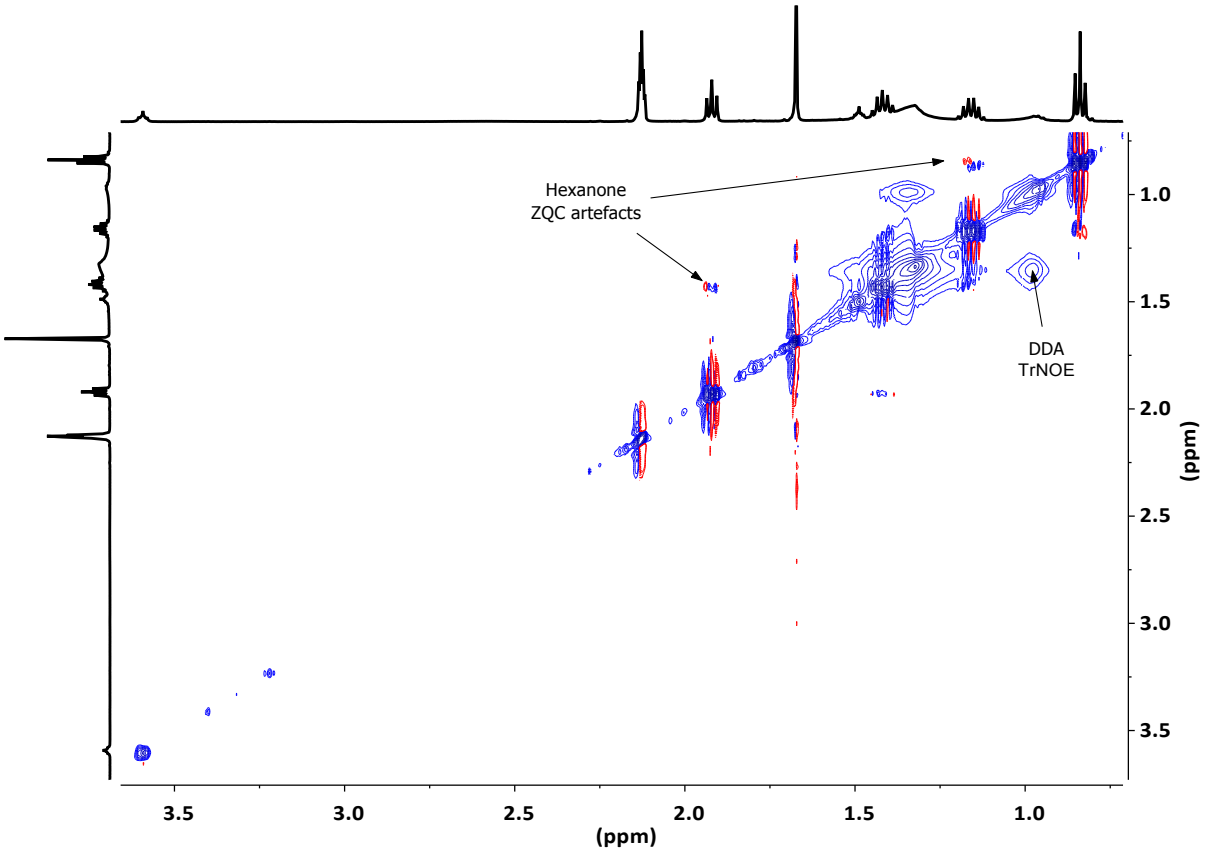

Figure SI 32: ^{1}H NOESY NMR spectrum (mixing time 100 ms) in Tol-d_8 of ZnO/DDA after the addition of HONE.

References

1 Z. Zhao, Z. Zheng, C. Roux, C. Delmas, J.-D. Marty, M. L. Kahn, C. Mingotaud, *Chem. Eur. J.,* 2016, **22**, 12424-12429.

2 See for examples : (a) E.A. Meulenkamp, *J. Phys. Chem. B*, 1998, **102**, 5566-5572; (b) L. Zhang, L. Yin, C. Wang, N. Iun, Y. Qi, D. Xiang, *J. Phys. Chem. C*, 2010, **114**, 9651-9658.

3 N. McCann, D. Phan, X. Wang, W. Conway, R. Burns, M. Attalla, G. Puxty, M. Maeder, *J. Phys. Chem. A* 2009, **113***,* 5022-5029.

4 Y. Coppel, G. Spataro, C. Pages, B. Chaudret, A. Maisonnat, M. L. Kahn, *Chem. Eur. J.*, 2012, **18**, 5384-5393.